Are upwelling systems an underestimated source of omega-3 in the ocean? The case of the southern Benguela upwelling system

Eleonora Puccinelli[1,2,3], Sarah E. Fawcett[3,4], Raquel F. Flynn[3], Jessica M. Burger[3], Gaspard Delebecq[2], Nolwenn Duquesne[2], Christophe Lambert[2], Hazel Little[3], Laure Pecquerie[2], Fany Sardenne[2], Sina Wallschuss[3], Philippe Soudant[2]

[1] Department of Coastal Systems, Royal Netherlands Institute for Sea Research (NIOZ), Texel, The Netherlands

[2] University of Brest- UMR 6539 CNRS / UBO / IRD / Ifremer, LEMAR - IUEM – Rue Dumont d' Urville - 29280 – Plouzané, France

[3] Department of Oceanography, University of Cape Town, Rondebosch 7701, Cape Town, South Africa

[4] Marine and Antarctic Research Centre for Innovation and Sustainability (MARIS), University of Cape Town, Rondebosch 7701, Cape Town, South Africa

Corresponding author: eleonora.puccinelli@nioz.nl, ORCID: 0000-0002-6144-6650

Key Points:

- Upwelling promoted phytoplankton omega-3 production, which was tightly coupled to the introduction of new-nitrogen during upwelling
- Pre-upwelling, non-diatom trophic markers were dominant, with a rapid switch within just two days to diatom trophic markers post-upwelling
- Omega-3 concentrations were 10-times higher than previous reports, suggesting that global omega-3 production is largely underestimated

Abstract

The Benguela Upwelling System (BUS) is one of the world's most productive ecosystems, supporting globally relevant pelagic fisheries. BUS marine community can change as a function of nutrients and omega-3 long chain polyunsaturated fatty acids (hereafter, omega-3) availability. Phytoplankton growth is supported by upwelled nitrate, a new source of nitrogen (N), or by recycled N forms such as ammonium. Preferential assimilation of one N form over another may lead to differences in omega-3 production between high and low food-quality species. This study evaluates how upwelling and the N source(s) used by phytoplankton influence omega-3 production. Sampling was conducted in the BUS at an anchor station sampled daily for 10 consecutive days. An upwelling event on days 5-6-7 supplied high concentrations of nutrients to surface waters, while pre- and post- upwelling the water column was well-stratified with low nutrient concentrations. Omega-3 and phytoplankton concentrations declined to ~zero during the upwelling event. Nanoplankton (2.7-10μm) were responsible for most of the productivity (30-95%) and relied on nitrate for their growth. Omega-3 concentrations at the surface reached peaks of 215.5 and 175.3μgL^{-1} pre- and post-upwelling, which were up to 10-times higher than previous measurements from the BUS. Pre-upwelling, non-diatom trophic markers were dominant, with a rapid switch (over just two days) to diatom trophic markers post-upwelling. This study defines the key role of upwelling in promoting phytoplankton omega-3 production, which is tightly coupled to the introduction of new-N during upwelling. The high concentrations of omega-3 reported suggest that global omega-3 production is largely underestimated.

Plain Language Summary

Omega-3 are fatty acids commonly found in several kind of food (e.g., fish), and are also extremely important for human health. Human and most animals however, cannot produce omega-3 in sufficient quantity to satisfy their health requirements and must thus acquire them through the diet. In the ocean, the main source of omega-3 is represented by phytoplankton

with different species being able to produce a different quantity and kind of omega-3. Phytoplankton growth is also dependent on nutrient availability, including nitrogen (N), and assimilation of a new source of N such as upwelled-nitrate or a recycled source such as ammonium, may lead to a phytoplankton community that produce different amounts of omega-3. This study evaluates how upwelling and the N source(s) used by phytoplankton influence omega-3 production. From our 10-day investigation conducted off the west coast of South Africa, we found that upwelling promoted phytoplankton omega-3 production, and this community relied on upwelled-nitrate as main N source. The community compositions changed rapidly during the investigation, which was reflected in the amount and kind of omega-3 produced. Generally, the concentrations we found were 10-times higher than previous measurements for the system, suggesting that the global omega-3 production is largely underestimated.

Key words: fatty acid, nitrogen cycling, food web, phytoplankton, productivity, nanoplankton

1. INTRODUCTION

Omega-3 long chain polyunsaturated fatty acids (hereafter omega-3) are essential nutritional components for all living organisms including humans and are sourced predominantly from fish and other seafood (Hicks et al., 2019; Tocher et al., 2019). Omega-3 have several essential roles, including maintaining membrane function (Parrish, 2013) and enhancing the growth, development and reproduction output of several organisms (e.g., Mourente, 2003; Garrido et al., 2007; Ravet et al., 2010), as well as constituting a major component of aquaculture feeds (Tacon & Metian, 2009; Tocher, 2015). In the ocean, the main producers of omega-3 are phytoplankton, while consumers are unable to synthetize omega-3 in sufficient quantities to meet their health requirements, such that omega-3 must be acquired through their diet (Arts et al., 2001; Dalsgaard et al., 2003; Litzow et al., 2006). Plankton community composition is the main factor regulating the amount of omega-3 produced by a given system (Galloway & Winder, 2015; Cañavate, 2019; Jónasdóttir, 2019). Diatoms, dinoflagellates and haptophytes are considered high food-quality species, producing high amounts of omega-3, in particular eicosapentaenoic-acid (20:5n-3, EPA) by diatoms and docosahexaenoic-acid (22:6n-3, DHA) by the latter two groups (Dalsgaard et al., 2003; Remize et al., 2020). In contrast, low food-quality species, such as cyanobacteria and chlorophyceae, yield low amounts of omega-3 and instead produce mostly short-chain polyunsaturated FA (PUFA) (i.e., ≤C18 PUFA; Cañavate, 2019).

The Benguela upwelling system (BUS) off the western coast of Southern Africa is one of the four major Eastern Boundary Upwelling Systems (EBUS), which together cover only 2 % of global ocean area while supporting 8 % of marine primary production and almost 20 % of the global marine fish catch (Pauly & Christensen, 1995). As such, EBUS support many of the world's most important pelagic fisheries (e.g., small-pelagic fisheries; Cury & Roy, 1989; Ward et al., 2006). The BUS is divided into two subsystems, the northern and southern BUS (NBUS and SBUS, respectively), separated by a permanent upwelling cell located off Lüderitz (Hutchings et al., 2009), and both supports high rates of primary and secondary

production (Shannon, 1985; Huggett et al., 2009; Flynn et al., 2020). Upwelling favors phytoplankton production through a succession of known producers of high amounts of omega-3, with communities dominated first by diatoms and then by dinoflagellates/haptophytes (Pitcher et al., 1991; Puccinelli, et al., 2016b; Burger et al., 2020). As such, EBUS may represent hot-spot regions for omega-3 production.

In EBUS, nitrate (NO_3^-) upwelled from depth is the main nitrogen (N) source fuelling primary production (supporting "new production") and has been estimated to support over 50% of phytoplankton growth (Waldron & Probyn, 1992; Messié et al., 2009; González-Galisteo et al., 2019). The higher-than-average concentrations of iron that are supplied to surface waters by upwelling lead to the preferential consumption by phytoplankton of upwelled NO_3^- over recycled N forms (e.g., ammonium (NH_4^+)), the consumption of which supports "regenerated production" (Dugdale & Goering, 1967). NO_3^- assimilation usually promotes the growth of large phytoplankton including diatoms (Kudela & Dugdale, 2000; Fawcett & Ward, 2011), while smaller phytoplankton including cyanobacteria tend to utilise NH_4^+ (Probyn & Painting, 1985; Fawcett et al., 2011). It is therefore possible that the assimilation of one N source over another (i.e., NO_3^- over regenerated N), each of which is associated with a different phytoplankton community, will be reflected in omega-3 production in a particular system.

Recent studies have indicated that the global supply of omega-3 is declining, with current predictions indicating that the supply will soon become insufficient for the growing human population (Hixson & Arts, 2016; Colombo et al., 2020), Indeed, it has been estimated that of the 1.4 Mt annual requirement of EPA+DHA, only 0.8 Mt are currently available (Hamilton et al., 2020). Moreover, 90% of the global phytoplankton EPA+DHA supply is thought to be lost between primary producers and higher trophic levels (Hamilton et al., 2020). However, information on the omega-3 supply from upwelling systems remains scarce (Puccinelli et al., 2021).

With a specific focus on the SBUS, the broad objective of this work is to improve our knowledge of omega-3 production in upwelling systems. This study aims first to i) determine the main source(s) of N used by phytoplankton during upwelling and then ii) evaluate the amount of omega-3 produced by these phytoplankton that is ultimately available for higher trophic levels.

2. MATERIAL AND METHODS

2.1. Study area and sampling design

Sampling took place aboard the MA-RE1 7.3 m Gemini inflatable craft over 10 consecutive days in late austral summer (11th-20th March 2020) during the upwelling season at an anchor station site in Elandsbaai in the SBUS (32.308°S; 18.275°E; bottom depth of ~30m; Burger et al., 2020) (Fig 1).

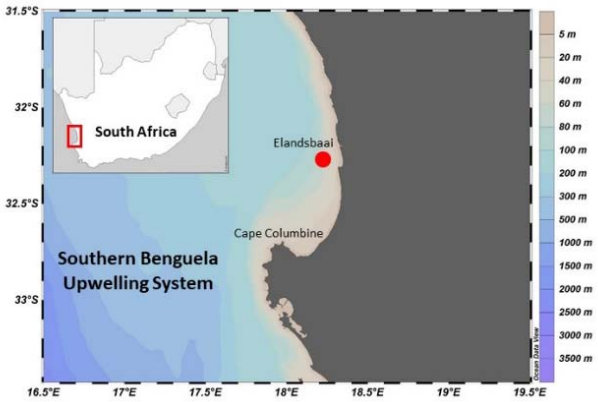

Fig 1 Map of the study area in the southern Benguela upwelling system showing the location of the anchor station in Elandsbaai (red dot) where the study was conducted. The coloured shading indicates bathymetry (m).

Upwelling in the SBUS is wind-driven and occurs seasonally, predominantly during austral summer (Shannon & Nelson, 1996; Hutchings et al., 2009). Wind-driven upwelling events in the vicinity of Cape Columbine (see Fig 1 for location) supply cold, nutrient-rich Subantarctic Mode Water (SAMW) to the surface (Lamont et al., 2015; Flynn et al., 2020), which is then advected northwards, including into Elandsbaai (Bailey & Chapman, 1991).

142 Such events result in the mixing of the water column in Elandsbaai and the advection of
143 nutrients into the surface layer.

144 Wind data between the 15th of February and 15th of April 2020 were used to investigate
145 the potential for upwelling events in the sampling region before and after sampling (Table
146 S.1). During the 10-day experiment, seawater samples were collected daily using a hand-held
147 5L Niskin bottle from seven depths over the water column: surface (0 m), sub-surface (5 m),
148 deep (10 m, 15 m, 20 m, 25 m and bottom ~ 30 m), unless otherwise specified. Hydrographic
149 data (temperature and salinity) were generated using a Seabird conductivity-temperature-
150 depth (CTD) profiler. The mixed layer depth (MLD; m) was determined from potential
151 density derived from CTD temperature and salinity following de Boyer Montegut et al.
152 (2004). The diffuse attenuation coefficient of photosynthetically active radiation (Kd(PAR))
153 was estimated using a Secchi disk (Idso and Gilbert, 1974; Table S.2) and then used to
154 estimate the depth of the euphotic zone (Zeu, m; (Kirk, 1994).

155 **2.2.Sample collection**

156 Seawater samples were collected for the analysis of oxygen, nutrient- (nitrate, nitrite,
157 ammonium, phosphate, silicic acid) and chlorophyll *a* concentrations, phytoplankton
158 taxonomy and flow cytometry, nitrate isotope ratios, stable isotopes (SI) of particulate
159 organic matter (N and C), rates of net primary productivity (NPP) and N (as NO_3^- and NH_4^+)
160 uptake, and phytoplankton fatty acid composition.

161 ***2.2.1. Oxygen and nutrient concentrations***

162 Duplicate seawater samples for oxygen analysis were collected in Biological Oxygen
163 Demand (BOD) bottles and immediately fixed and stored in the dark until analysis, which
164 occurred less than 5hr later. In the laboratory, the dissolved oxygen concentrations were
165 measured using the Winkler titration method (Carpenter, 1965; Grasshoff, 1976).

166 Nutrients were collected in duplicate in 50 mL Falcon tubes and frozen at -20°C until
167 analysis. Nitrate + nitrite and silicic acid concentrations ($[(NO_3^- + NO_2^-)]$ and $[Si(OH)_4]$)
168 were measured using a Lachat QuickChem flow injection analysis platform (Grasshoff, 1976;

Diamond, 1994). The detection limit for both nutrients was 0.1 µM. Phosphate and nitrite concentrations ($[PO_4^{3-}]$ and $[NO_2^-]$) were measured manually using standard colorimetric methods (Parsons et al., 1984), with a detection limit of 0.05 µM. The NO_3^- concentrations were calculated by subtracting $[NO_2^-]$ from $[NO_3^-+NO_2^-]$. Aliquots of a certified reference material (CRM; JAMSTEC; Lot CG) were analysed during auto-analyser and manual runs to ensure measurement accuracy. The fluorometric method (Holmes et al., 1999) was used to analyse NH_4^+ concentrations ($[NH_4^+]$), with a detection limit of 0.05 µM. The $[NH_4^+]$ measurements were corrected for the matrix effect (ME) (Saxberg & Kowalski, 1979).

2.2.2. Chlorophyll a and phytoplankton taxonomy

Seawater (1 L from each depth) was collected in opaque high-density polyethylene bottles for chlorophyll *a* analysis. From each depth, 300 mL of seawater was filtered through a combusted (all glass fibre filters (GF/F) were ashed at 450ºC for 5hr) 0.3 µm GF/F, 300 mL through a 2.7 µm GF/F, and the remaining 400 mL through a 10 µm nylon mesh for the determination of chlorophyll *a* concentrations of different phytoplankton size classes (picoplankton: 0.3-2.7 µm; nanoplankton: 2.7-10 µm; microplankton: >10 µm). The chlorophyll *a* on each filter was extracted in 90 % acetone for 24hr at -20ºC in the dark, after which fluorescence was determined following Welschmeyer (1994). The chlorophyll *a* concentrations ([Chl *a*]) of the pico- and nanoplankton were then determined by subtraction: $[\text{Chl } a]_{\text{picoplankton}}$ = [Chl *a*] on the 0.3 µm filter – [Chl *a*] on the 2.7 µm filter; $[\text{Chl } a]_{\text{nanoplankton}}$ = [Chl*a*] on the 2.7 µm filter – [Chl *a*] on the 10 µm filter. The microplankton [Chl *a*] was taken to be the [Chl *a*] on the 10 µm filter.

Two approaches were used to investigate phytoplankton community compositions. For identification and enumeration of larger phytoplankton, samples were collected using a plankton net (50 µm mesh size and 25 cm diameter) deployed at 5 m (total volume of water filtered ~245 L). The contents were transferred to a Falcon tube and immediately fixed with 200 µL of a 25 % glutaraldehyde solution. Phytoplankton were enumerated from subsamples

using an inverted microscope (640 x magnification), with identification to the highest taxonomic level possible.

For identification and enumeration of the smaller phytoplankton community, triplicate seawater samples (2 mL) were collected in cryovials and immediately fixed with 20 µL of a glutaraldehyde solution (glutaraldehyde 0.3 % final concentration) for flow cytometry (FC), then frozen at -80°C until analysis. The following phytoplankton groups were identified (FC-picoplankton (~0.5- <3 µm), FC-nanoplankton (~2-20 µm), *Synechococcus*-like cells (~1-3 µm), and cryptophyte-like cells (~10-30 µm)). Green-fluorescent polystyrene bead solution ("Flow Check", Polyscience, 1 % in sterile 0.2 µm filtered seawater) was used as the internal standard. Results are expressed as cellmL^{-1}. The biovolume of each group was calculated following Bouvier et al. (2001).

2.2.3. Nitrate isotopes

The $\delta^{15}N$ ($\delta^{15}N$, in ‰ vs. N_2 in air, = $[(^{15}N/^{14}N)_{sample}/(^{15}N/^{14}N)_{ref} -1] \times 1000$) and $\delta^{18}O$ ($\delta^{18}O$, in ‰ vs. VSMOW, = $[(^{18}O/^{16}O)_{sample}/(^{18}O/^{16}O)_{ref} -1] \times 1000$) of seawater nitrate ($\delta^{15}N_{NO3}$ and $\delta^{18}O_{NO3}$) were measured using the denitrifier method (Sigman et al., 2001; Casciotti et al., 2002). Prior to isotopic analysis, samples were treated with sulfamic acid to remove NO_2^- (Granger & Sigman, 2009; Fawcett et al., 2015). The N and O isotope ratios of the N_2O were measured using a Delta V Advantage isotope ratio mass spectrometer (IRMS). Results were referenced to atmospheric N_2 and VSMOW using the CRMs, IAEA-NO-3 ($\delta^{15}N$ = 4.7 ± 0.2‰; Gonfiantini et al., 1995 and $\delta^{18}O$ = 25.6 ± 0.4‰; Böhlke et al., 2003) and USGS-34 ($\delta^{15}N$ = -1.8 ± 0.1‰ and $\delta^{18}O$ = -27.9 ± 0.3‰; Böhlke et al., 2003). The analytical precision for repeat $\delta^{15}N_{NO3}$ and $\delta^{18}O_{NO3}$ measurements was ≤0.1‰ and ≤0.2‰, respectively.

2.2.4. Particulate organic matter

Seawater (1L from each depth) was collected in opaque high-density polyethylene bottles for particulate organic N (PON) and carbon (POC) analysis following pre-filtration through a 200 µm mesh to remove large grazers. At each depth, as per the chlorophyll *a* analyses, 300 mL of seawater was filtered through a 0.3 µm GF/F, 300 mL through a 2.7 µm GF/F, and the

222 remaining 400 mL through a 10 μm nylon mesh. The material on the 10 μm nylon mesh was
223 re-suspended in filtered seawater (<0.2 μm), then collected on a 0.3 μm GF/F Filters were
224 stored in ashed foil at -20°C pending analysis.

225 In the laboratory, filters were oven-dried at 40°C for 24hr and pelletised in tin capsules.
226 Samples were analysed for PON and POC content and $\delta^{15}N$ and $\delta^{13}C$ using a Flash Elemental
227 Analyzer 1112 Series coupled to a Delta V Plus IRMS. A protocol blank (unused pre-
228 combusted filter + tin capsule) was run after every 10-20 samples and laboratory standards
229 calibrated to IAEA CRMs were run after every five samples. The detection limit was 2 μg C
230 and 1μg N, and analytical precision was <0.1‰ for $\delta^{13}C$ and $\delta^{15}N$. The PON and POC of the
231 pico- and nanoplankton size classes was calculated by subtraction as for chlorophyll *a*. Their
232 $\delta^{15}N$ and $\delta^{13}C$ were then calculated, accounting for the concentration of PON and POC in
233 each size class: $\delta^{15}N$ or $\delta^{13}C$ picoplankton = [($\delta^{15}N$ or $\delta^{13}C$ x PON or POC on the 0.3 μm
234 filter) – ($\delta^{15}N$ or $\delta^{13}C$ x PON or POC on the 2.7 μm filter)] / (PON or POC on the 0.3 μm
235 filter – PON or POC on the 2.7 μm filter); $\delta^{15}N$ or $\delta^{13}C$ nanoplankton = [($\delta^{15}N$ or $\delta^{13}C$ x PON
236 or POC 2.7 μm filter) – ($\delta^{15}N$ or $\delta^{13}C$ x PON or POC 10 μm filter)] / (PON or POC 2.7 μm
237 filter – PON or POC 10 μm filter). The $\delta^{15}N$ or $\delta^{13}C$ of microplankton (>10 μm) was
238 represented by the measured $\delta^{15}N$ or $\delta^{13}C$ of the 10 μm filter.

239 ***2.2.5. Rates of NPP and N uptake***

240 Daily simulated *in situ* experiments were conducted to determine the rates (μM h^{-1}) of C
241 fixation (NPP) and N uptake (as NO_3^- and NH_4^+; ρNO_3^- and ρNH_4^+) at five depths: 0 m, 5 m,
242 10 m, 15 m and 20 m. At each depth, seawater was pre-filtered (200 μm) into four 1 L clear
243 polycarbonate bottles. Two bottles (duplicates) were amended with $K^{15}NO_3$ and $NaH^{13}CO_3$
244 (final ^{15}N- and ^{13}C concentration of 0.5 μM and 100 μM, respectively) and two bottles with
245 $^{15}NH_4Cl$ (final ^{15}N concentration of 0.05 μM). Bottles were incubated *in situ* for 4hr by
246 attaching them to an anchored rope, with each bottle fastened at its depth of collection.
247 Experiments were terminated via filtration of the 1L bottle contents: 300 mL through a 0.3
248 μm GF/F, 300 mL through a 2.7 μm GF/F, and 400 mL through a 10 μm nylon mesh. The

material on the 10 μm nylon mesh was re-suspended in filtered seawater (<0.2 μm), then collected on a 0.3 μm GF/F. Filters were stored in ashed foil at -20°C until analysis. The incubation filters were analysed for PON and POC content and N and C isotopes as described for the PON and POC samples. NPP, ρNO_3^- and ρNH_4^+ were then calculated following Dugdale and Wilkerson (1986):

Equation 1: $$\rho_x = \left(\frac{(R_{xs})}{((R_{enr})-(F)) \times T}\right) \times \text{PON or POC}$$

where x is C, NH_4^+ or NO_3^-; R_{xs} is the measured ^{15}N or ^{13}C atom % in the PON or POC minus the natural abundance atom % (F, = 0.366 % for ^{15}N and 1.07 % for ^{13}C), R_{enr} is the atom % of ^{15}N or ^{13}C in the incubation seawater directly following tracer addition (calculated for ^{15}N and assumed for ^{13}C to be 5%), and T is the incubation length (hr). The NPP, ρNO_3^- and ρNH_4^+ associated with the pico- and nanoplankton were calculated by subtraction as for the chlorophyll *a*, PON and POC, with the microplankton rates derived from the material collected on the 10μm filters.

2.2.6. Fatty acids

Seawater (4 L) for FA analysis was pre-filtered (200 μm) and collected in triplicate from four depths: 0 m, 5 m, 10 m and 30 m. The seawater was filtered through 0.3 μm GF/F, then immediately stored in liquid nitrogen and subsequently at -80°C until analysis. Samples were lyophilised for 48hr upon arrival in the laboratory.

Lipids were extracted using a modification of the Folch et al. (1957) procedure through homogenisation in 6mL of a fresh solution of methanol and chloroform (2/1; v/v) and closed under N_2 atmosphere. FA methyl esters (FAME) were obtained after acidic transesterification by the addition of a H_2SO_4/methanol solution (3.4 %; v/v) and heating at 100°C for 10min. FAME composition was determined using a Varian CP8400 Gas Chromatograph equipped with a ZBWAX column with hydrogen as the carrier gas. Peaks were identified by comparison with retention times of external standards (Supelco37, PUFA No.1 and No.3, Bacterial Acid Methyl Ester Mix; Sigma). FAME peak area was converted into μg of FA

based on the peak area of the internal standard (23:0). Concentrations are expressed in μgL^{-1}. FA are reported using the notation A:Bn-*x*, where A is the number of carbon atoms, B is the number of double bonds, and *x* indicates the position of the first double bond relative to the terminal methyl group (Puccinelli et al., 2016 b). Among the common FA trophic markers (TM), omega-3 constitutes the sum of long chain n-3, including 20:3n-3, 20:4n-3, 20:5n-3, 21:5n-3, 22:5n-3 and 22:6n-3. The sum of 16:1n-7, 16:2n-4, 16:2n-7,16:3n-4, 16:4n-1 was used as a diatom TM and the sum of 18:1n-9, 18:4n-3, 18:5n-3 as a non-diatom TM (i.e., haptophyte/dinoflagellate; Parrish et al., 2000). The ratio of EPA/DHA can be used to identify communities mostly supported by non-diatoms (ratio<1) or by diatoms (ratio>1) (Dalsgaard et al., 2003). The FA data were also used to estimate the nutritional quality of phytoplankton for higher trophic levels using the FA-based nutritional quality index (NQI) developed by Cañavate (2019). The NQI was calculated as follows:

Equation 2: $$\mathrm{NQI} = [(15 * \mathrm{DHA} + 10 * \mathrm{EPA} + 2 * \mathrm{ARA}) * 0.8 + (1.8 * \Sigma\mathrm{C18PUFA})] * \log(\frac{\mathrm{n-3}}{\mathrm{n-6}})$$

Where DHA, EPA and ARA (20:4n-6) are expressed as % of total FA (TFA). ΣC18PUFA is the sum of the 18:2n-4, 18:2n-6, 18:3n-1, 18:3n-2, 18:3n-3, 18:4n-3, 18:3n-6, 18:4n-1, 8:4n-3, 18:4n-6 and 18:5n-3 percentages, while n-3/n-6 is the ratio of n-3 PUFA to n-6 PUFA.

2.3.Data analysis

A multivariate permutational analysis (PERMANOVA; Anderson & Clarke, 2008) was performed to test for differences in the phytoplankton FA composition with depth (n=4) and day (n=10). Canonical analyses of principal coordinates (CAP) were used to explore differences in the phytoplankton FA composition between *Depth* and *Day*, focussing on the 0m and 5m where most of the FA were recorded. FA analyses were based on Euclidian dissimilarities calculated from percentage data. The analyses were conducted using the PERMANOVA+ add-on package of PRIMER v6 (Anderson & Clarke, 2008).

3. RESULTS

3.1. Hydrography

The upper water column (~5-10 m) was well stratified over much of the sampling period, except on days 5, 6 and 7 when an upwelling event occurred. During these three days, a decrease in temperature, density, oxygen and chlorophyll *a* concentrations was observed, coincident with an increase in the NO_3^- concentration (Fig 2, 3a and 4a-c). Pre- and post-upwelling, surface temperature (0m) was >17°C, dropping as low as 13°C during upwelling, while oxygen concentrations decreased from 360 µM pre- upwelling to a minimum of 220 µM during upwelling (Fig 2, Table S.3).

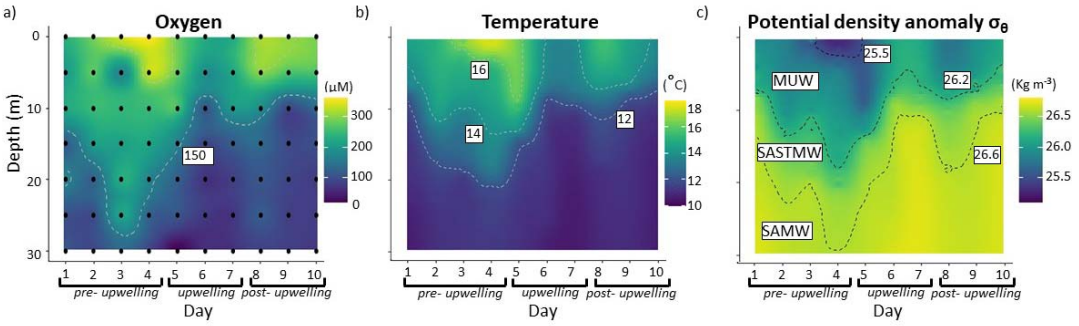

Fig 2 Vertical profiles of a) oxygen concentrations, b) temperature, and c) the potential density anomaly (σ_θ) sampled over 10 consecutive days at the anchor station in the southern Benguela upwelling system in March 2020. The black dots in panel a show the discrete sampling depth. The dashed black lines in panel c indicate the isopycnals separating the main water masses present in the study region: Subantarctic Mode Water (SAMW), South Atlantic Subtropical Mode Water (SASTMW) and Modified Upwelled Water (MUW).

The wind direction during the 10-day investigation was variable; however, south-south-westerly winds were the most prevalent. These winds were also prevalent for the months prior to and after the study period (Table S.1). Wind speed was significantly higher on days 5, 6 and 9 (4.9, 3.6 and 3.6 m s^{-1}, respectively) than on the other days (speed <3 m s^{-1}). Additionally, high wind speeds were recorded 12 days and three days prior to the study period (6.1 m s^{-1} and 4.1 m s^{-1}, respectively).

3.2.Nutrient concentrations

The nutrient profiles followed the same temporal pattern as the physical parameters (Figs 2 and S.1, Table S.3). Pre- and post- upwelling, most nutrient concentrations were higher

below the mixed layer (>5-10 m), with [NO_3^-] and [$Si(OH)_4$] as high as 27.9 µM and 30.0 µM, and [PO_4^{3-}] and [NO_2^-] reaching 3.0 µM and 1.4µ M, respectively. During the upwelling period, mixed-layer nutrient concentrations were elevated, with the highest surface concentrations measured on day 7, of 14.9 µM (NO_3^-), 13.1 µM (SiO_4^-), 3.0 µM (PO_4^{3-}) and 1.5 µM (NO_2^-). The [NH_4^+] showed a different trend from the other nutrients. While [NH_4^+] was generally low (<2 µM) throughout the study, water-column concentrations were higher during the non-upwelling period (maximum of 1.9 µM at 20 m on day 4). Maximum surface (<5 m) [NH_4^+] was measured during upwelling on day 6 (1.8 µM), while the lowest values were measured on days 7 and 10 (<0.1 µM).

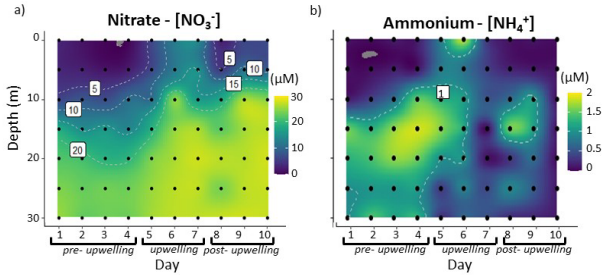

Fig 3 Vertical profiles of a) nitrate (NO_3^-) and b) ammonium (NH_4^+) concentrations for samples collected over 10 consecutive days at the anchor station in the southern Benguela upwelling system in March 2020.

3.3.Chlorophyll *a* and phytoplankton community composition

The chlorophyll *a* concentrations were dominated by the nanoplankton throughout the study, followed by the microplankton and picoplankton (Fig 4a-c). Nanoplankton showed the highest chlorophyll *a* concentrations pre- and post- upwelling at 0m and 5m (5.6 ± 0.3 µg L^{-1}; 68.5 ± 17.4 % of total chlorophyll *a*), with nanoplankton chlorophyll *a* decreasing to <2.6µgL^{-1} during the upwelling event. Microplankton showed low chlorophyll *a* concentrations pre- and during upwelling (0.9 ± 0.2 µg L^{-1}; 15.0 ± 7.2 %), which increased post- upwelling to 3.6 ± 0.3 µg L^{-1} (25.6 ± 10.6 %). Picoplankton contributed least to total chlorophyll *a*, with low concentrations throughout the investigation (0.2 ± 0.1 µg L^{-1}; 11.2 ± 5.3 %).

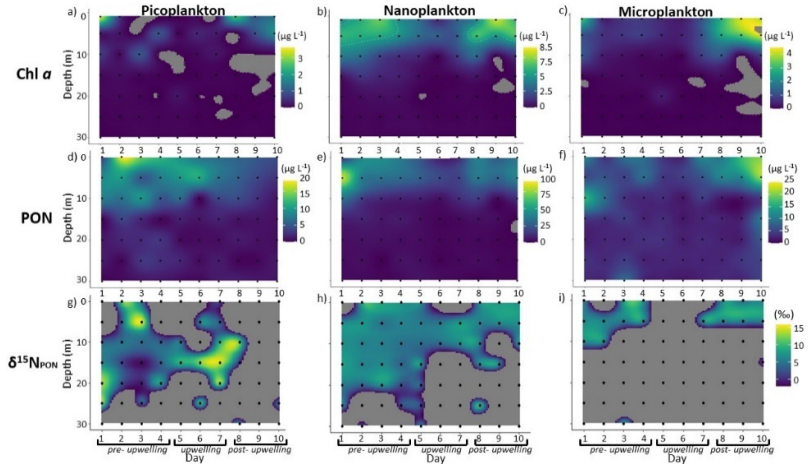

Fig 4 Profiles of picoplankton (0.3-2.7 µm), nanoplankton (2.7-10 µm) and microplankton (> 10µm) a-c) chlorophyll *a* concentrations, d-f) particulate organic nitrogen (PON) concentrations and g-i) $\delta^{15}N_{PON}$ for samples collected over 10 consecutive days at the anchor station in the southern Benguela upwelling system in March 2020. The grey shading indicates depths and days where concentrations and $\delta^{15}N_{PON}$ were below the methodological detection limits. The black dots indicate discrete sampling depths. We note that the colour bar is the same for panels g-i.

Microscopy analyses (phytoplankton >50 µm) indicated differences in phytoplankton abundances in the pre- (4.5 ± 2.2 10^4 cell L^{-1}), during (33.8 ± 19.7 10^4 cell L^{-1}) and post-upwelling (103.0 ± 63.4 10^4 cell L^{-1}) samples, with the highest abundances measured post-upwelling (228.2 10^4 cell L^{-1} on day 9). Apart from day 1 when samples contained near-exclusively dinoflagellates (>90 % total cell count), diatoms dominated the phytoplankton assemblage throughout the study period, with *Chaetoceros* spp. and *Pseudo-nitzschia* spp. being the most abundant species (Fig 5, Table S.4a).

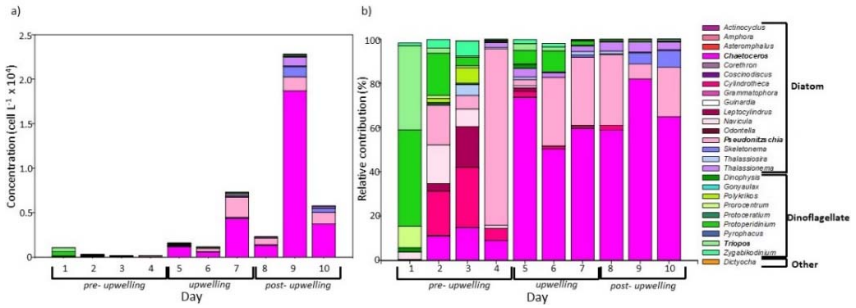

Fig 5 a) Cell counts (cellL^{-1}) and b) relative contributions (% of total cells counted) of the various phytoplankton species identified via light microscopy over 10 consecutive days at the anchor station in the southern Benguela upwelling system in March 2020. The most common diatoms (*Chaetoceros* spp., *Pseudo-nitzschia* spp.) and dinoflagellates (*Triopos* spp., *Protoperidinium* spp.) are highlighted in bold in the figure legend.

373 Flow cytometry analyses indicated that heterotrophic bacteria were the most abundant
374 small plankton group (0.5-3 μm) present throughout the investigation, with particularly high
375 abundances pre- and during upwelling on days 4 and 5 (maximum of 9 10^6 cell ml^{-1}). This
376 group was followed by *Synechococcus*-like cells, which were particularly abundant on days
377 2, 3 and 4 (pre- upwelling) between the surface and 10 m ($2.4 \pm 1.2 \times 10^4$ cell ml^{-1}; 63.9 ± 8.5
378 % of FC cells counted; Fig S.2, Table S.4b). FC-picoplankton, FC-nanoplankton and
379 cryptophyte-like cells were generally less abundant (<1.8 10^3 cell ml^{-1}; <37 % of FC cells
380 counted), although FC-nanoplankton had higher concentrations pre- upwelling compared to
381 during and post- upwelling (1.1 ± 0.5 10^3 vs. 4.8 ± 2.8 10^2 cellml^{-1}; 22.1 ± 8.2 vs. 13.0 ± 6.2
382 %). The biovolume was dominated by cryptophytes-like cells pre- and during upwelling
383 (maximum of 4.9 10^3 μm^3; 90 % of total biovolume of FC cells counted) and by FC-
384 nanoplankton post- upwelling (maximum of 3.0 10^2 μm^3; 99 %), with all other groups
385 contributing minimally (Fig S.2, Table S.4 b).

386 **3.4.Isotopes of nitrate and particulate organic matter**

387 As for the other parameters, $\delta^{15}N_{NO3}$ was clearly different pre-, during and post-
388 upwelling, and varied significantly with depth (Fig S.3, Table S.5). The highest $\delta^{15}N_{NO3}$ was
389 measured at the surface and 5m pre- and post- upwelling (11.9 ± 2.6‰). At all other depths
390 and at the surface during the upwelling event, the average $\delta^{15}N_{NO3}$ was 7.3 ± 0.9‰. $\delta^{18}O_{NO3}$
391 followed the same trend as $\delta^{15}N_{NO3}$, with values of 12.5 ± 3.4‰ observed pre- and post-
392 upwelling at the surface vs. 5.8 ± 1.3‰ at depth on all days, as well as at the surface during
393 upwelling.

394 The majority of the PON was attributed to nanoplankton, while micro- and picoplankton
395 contributed minimally (<25 μgL^{-1} of N; Fig 4d-f, Table S.5). Nanoplankton PON
396 concentrations were particularly high at the surface and subsurface (i.e., 0 m and 5 m) pre-
397 and post- upwelling, in contrast to at the other depths and during upwelling (41.9 ± 4.4 vs.
398 6.7 ± 0.1 μgL^{-1} of N). The $\delta^{15}N_{PON}$ of the nanoplankton averaged 6.9 ± 0.3‰ pre- and post-
399 upwelling vs. 5.4 ± 0.3‰ during upwelling. The picoplankton PON had a relatively high

400 $\delta^{15}N_{PON}$ at depth during upwelling (peak of 15‰ on day 7); however, due to the low N
401 content of the samples, for most of the depths and days it was not possible to make reliable
402 $\delta^{15}N_{PON}$ measurements for both pico- and microplankton (Fig 4g-i).

403 As for PON, most of the POC was attributed to nanoplankton, with the highest
404 concentrations occurring pre- and post- upwelling at 0 m and 5 m (223.3 ± 27.4 vs. 41.6 ± 5.5
405 μgL^{-1} of C; Fig S.4, Table S.5). $\delta^{13}C_{POC}$ varied minimally among the phytoplankton size
406 classes, with microplankton showing slightly lower values than the two other classes (-22.2 ±
407 1.9‰ vs. -19.8 ± 2.7‰). There was no clear effect of upwelling on the $\delta^{13}C_{POC.}$

408 **3.5. Rates of N uptake and NPP**

409 The highest rates of N uptake and NPP were observed for the nanoplankton size class,
410 while pico- and microplankton contributed minimally, with their rates in most cases below
411 the methodological detection limit (ρNO_3^-<0.9 μMhr^{-1}; ρNH_4^+<0.1 μMhr^{-1}; NPP<1.2 μMhr^{-1};
412 Fig 6, Table S.6). As such, only the nanoplankton rate data are discussed in detail below (i.e.,
413 Fig 6b, e and h).

414 All the uptake rates varied with depth and were higher pre- and post- upwelling when the
415 water column was strongly stratified, with lower rates measured during active upwelling and
416 when the water column was weakly stratified (Fig 6). Throughout the study, ρNO_3^- was
417 generally higher than ρNH_4^+, with maximum measured rates of 1.7 and 0.3 μMhr^{-1},
418 respectively (Table S.6). ρNO_3^- reached a maximum pre- upwelling at the surface/subsurface
419 (<5 m), especially on day 1 (1.7 μMhr^{-1}) and day 3 (1.4 μMhr^{-1}). Post- upwelling surface and
420 5 m values of ρNO_3^- were generally low (<0.2 μMhr^{-1}), with rates for the deeper samples and
421 on the other days that were at or below the detection limit (Fig 6 b). ρNH_4^+ showed a slightly
422 different pattern from ρNO_3^- in relation to upwelling, with the highest rates measured at 0 m
423 (and in some cases at 5 m) throughout the investigation (0.2 ± 0.1 μMhr^{-1}) except on days 7-
424 8-9 when the surface and 5 m ρNH_4^+ decreased to 0.1 ± 0.0 μMhr^{-1} (Fig 6e). For the other
425 depths and days, ρNH_4^+ was either near or below the detection limit.

NPP was an order of magnitude higher pre- and post- upwelling at 0 m and 5 m compared to deeper samples and on the other days (2.9 ± 0.9 μMhr^{-1} vs. 0.2 ± 0.1 μMhr^{-1}). The maximum rate of NPP was recorded at the surface on day 1 (8.0 μMhr^{-1}) followed by surface measurements made on days 3 and 8 (both 5.1 μMhr^{-1}; Fig 6 h, Table S.6).

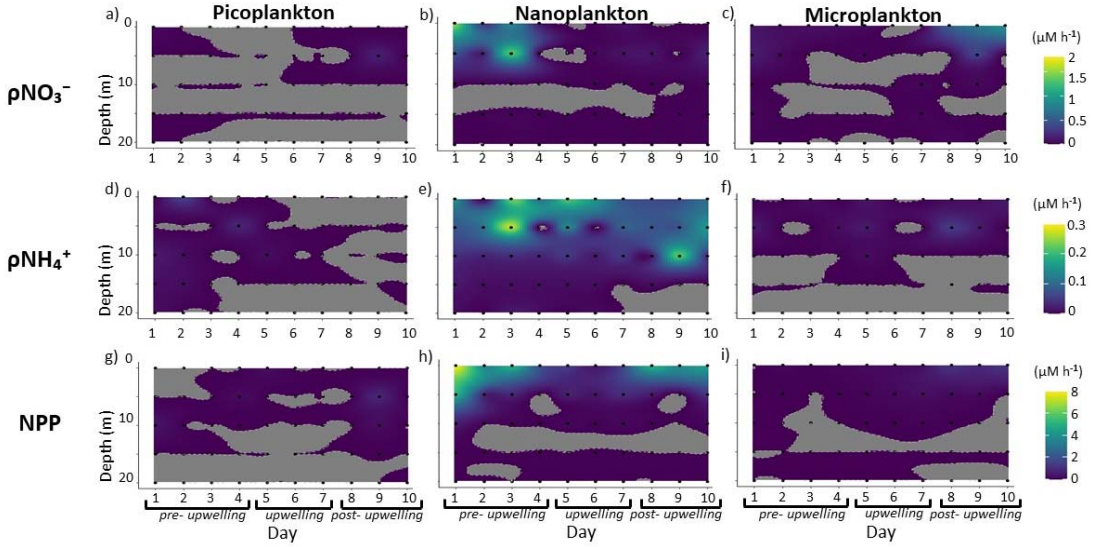

Fig 6 Size-fractionated (picoplankton, 0.3-2.7 µm; nanoplankton, 2.7-10 µm; microplankton, >10 µm) rates of a-c) nitrate uptake (ρNO_3^-), d-f) ammonium uptake (ρNH_4^+) and g-i) net primary production (NPP) measured at five depths (0 m, 5 m, 10 m, 15 m and 20 m) over 10 consecutive days at an anchor station in the southern Benguela upwelling system in March 2020. The grey shading indicates depths and days where the rates were below the methodological detection limit.

3.6.Fatty acids

The concentrations of phytoplankton TFA showed the same pre- and post- upwelling trends as the other parameters, with values during the upwelling event that were close to 0 μgL^{-1} throughout the water column (Fig 7, Table S.7). TFA concentrations were high at 0 m and 5 m pre- and post- upwelling, reaching maxima of 185.0 ± 35.4 μgL^{-1} and 148.0 ± 24.1 μgL^{-1}, respectively. These TFA maxima coincided with peaks in the total POC concentrations, which reached 429 and 240 μgL^{-1} pre- and post- upwelling, respectively. Omega-3 followed the same pattern, with the highest concentrations recorded at the surface on day 3 (49.5 ± 6.1 μgL^{-1}) and at 5m on days 8 and 9 (29.3 ± 2.2 μgL^{-1}). Most of TFA sampled pre- upwelling was attributed to non-diatom TM, such as ΣC18-PUFA (>50 % of TFA), in particular 18:5n-3, which alone represented up to 20 % of the TFA (Figs S.6 and

S.7). By contrast, post- upwelling diatom TM made up as much as 60 % of TFA and ΣC16-PUFA constituted 15 % of TFA. While 18:5n-3 was present predominantly pre-upwelling, 18:4n-3 was evenly distributed pre- and post-upwelling (Fig S.7, f and g). Peaks of TFA and omega-3 were also observed for the deepest samples on days 4, 5 and 10 (TFA 101.2 ± 6.1 μgL^{-1}, 79.8 ± 1.8 μgL^{-1}, 148.0 ± 24.2 μgL^{-1} respectively), with non-diatom TM dominating on days 4-5 and diatom TM on day 10 (Fig 7, Table S.7).

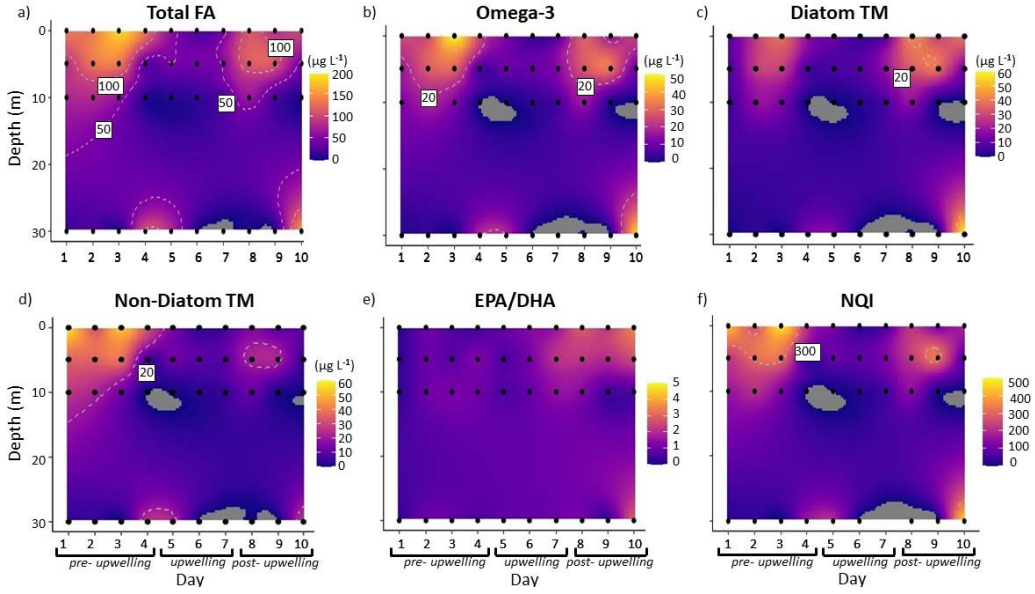

Fig 7 Fatty acid (FA) composition (μgL^{-1}) of phytoplankton samples collected from four depths (0 m, 5 m, 10 m, 30 m) over 10 consecutive days at an anchor station in the southern Benguela upwelling system in March 2020. a) Total FA, b) Omega-3 (20:3n-3, 20:4n-3, 20:5n-3, 21:5n-3, 22:5n-3, 22:6n-3), c) diatom TM (Trophic Markers :16:1n-7, 16:2n-4, 16:2n-7, 16:3n-4, 16:4n-1), d) non-diatom TM (18:3n-3, 18:4n-3, 18:5n-3), e) EPA/DHA (20:5n-3/22:6n-3), f) NQI = nutritional quality index (equation 2). The grey shading indicates depths and days where values were below the methodological detection limit.

The CAP analysis revealed a clear pattern of separation among samples collected pre-, during and post- upwelling, a trend ascribed to non-diatom TM pre- upwelling and diatom TM post- upwelling (Fig 8). The same trend was evident in the EPA/DHA ratio, which was significantly higher post- upwelling, indicating the presence of a phytoplankton community comprising mostly diatoms, with values of 0.7 ± 0.1, 1.3 ± 0.1, and 2.5 ± 0.1 for pre-, during and post- upwelling, respectively (Fig 7e, Table S.7).

The nutritional quality index (NQI) based on FA followed the same trend as the other parameters, with higher values at 0 m and 5 m pre- and post- upwelling (216.5 ± 15.3) compared to at the other depths and during upwelling (89.7 ± 13.5; Fig 7f, Table S.7). The exception to this pattern was the bottom water samples collected on days 4, 5 and 10 for which we derived NQI values of 157.8 ± 23.2, 244.5 ± 10.7 and 297.9 ± 24.8, respectively.

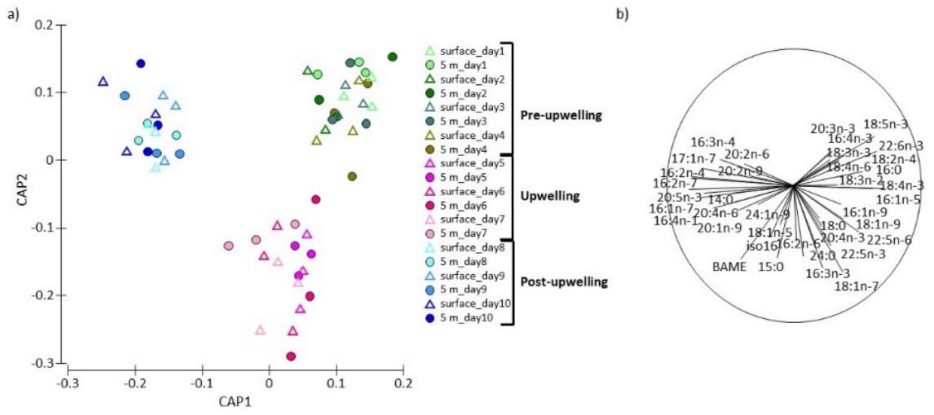

Fig 8 a) Canonical analysis of principal coordinates (CAP) performed on the fatty acid composition of phytoplankton samples collected over 10 consecutive days at an anchor station in the southern Benguela upwelling system in March 2020. Only 0 and 5 m samples were used for the analysis. Colour shading indicates different stages of upwelling, as indicated by the environmental data: green = pre- upwelling (days 1- 4), pink = during upwelling (days 5-7), blue = post- upwelling (days 8-10). Each symbol in panel a) represents a single sample. b) Distribution of eigenvalues for each factor (fatty acids). BAME = Bacterial Fatty Acids.

4. DISCUSSION

This study aimed to provide the first estimates of phytoplankton omega-3 concentrations for the SBUS and to investigate the potential role of N cycling in influencing their production. We found that omega-3 concentrations were extremely high at both 0m and 5m, pre- and post- upwelling, when the NO_3^- uptake rates reached a maximum. Furthermore, the omega-3 concentrations were much higher (~10 times) than the estimates currently available for the SBUS (Puccinelli et al., 2021). Below, we explore possible explanations for the upwelling related patterns that we observed and discuss the implications for omega-3 availability to higher trophic levels.

4.1. Upwelling event and the N sources available to phytoplankton

495 During the 10-day investigation, we recorded an upwelling event on days 5-6-7, which
496 drove a decrease in the mixed-layer temperature and oxygen concentration coincident with an
497 increase in the nutrient concentrations. This phase occurred between pre- (days 1-4) and post-
498 (days 8-10) upwelling periods that were associated with a well-stratified upper (~5 m) water
499 column and a shallow mixed layer, consistent with expectations for the SBUS during periods
500 of relaxation (Bailey & Chapman, 1991; Zhang et al., 2015; Aristizábal et al., 2017; Burger et
501 al., 2020). During the non-upwelling periods, NPP and chlorophyll *a* reached a maximum at
502 0m and 5m, facilitated by favourable conditions for phytoplankton growth, including high
503 nutrient- and light availability. The values recorded here (54.1 ± 12.1 μMd^{-1} and 6.8 ± 3.5
504 μgL^{-1} for NPP and chlorophyll *a*, respectively) are similar to previous observations made in
505 Elandsbaai in summer (45 μMd^{-1} and 9-15 μgL^{-1}; Pitcher et al., 1991; Burger et al., 2020),
506 with elevated phytoplankton productivity generally occurring immediately following the
507 cessation of upwelling (i.e., at the onset of relaxation), highlighting the pivotal role of the
508 upwelling cycle in modulating productivity in this region.
509 The two main N sources in the system, NO_3^- and NH_4^+, were delivered to surface waters
510 during upwelling, yielding a surface [NO_3^-] that was two-fold higher than the [NH_4^+] (Fig 2,
511 Table S.3). Elevated [NO_3^-] is typically supplied to the surface by the upwelling of SAMW,
512 the ultimate source of nutrients to the SBUS (Lamont et al., 2015; Flynn et al., 2020).
513 Additionally, in a shallow regions of the SBUS such as Elandsbaai (maximum depth of 30
514 m), nutrients (including NO_3^-) tend to accumulate in bottom waters during the non-upwelling
515 season as a result of stratification, high rates of remineralization, and water-mass retention
516 (i.e., "nutrient trapping"; Flynn et al., 2020); these nutrients are then supplied to the surface
517 layer when upwelling and/or wind-driven mixing ventilates the bottom waters. The higher
518 [NH_4^+] at the surface during the upwelling period can be also explained by water column
519 mixing given that [NH_4^+] was elevated at depth (1.5-2.0 μM at > 15m) during much of our
520 investigation. By contrast, [NH_4^+] was extremely low in surface waters pre- and post-
521 upwelling, presumably due to rapid NH_4^+ uptake by phytoplankton (Dortch, 1990) and the

522 fact that shallow stratification prevented its upward supply. The high [NH_4^+] at depth was
523 likely the result of NH_4^+ production in excess of it consumption during organic matter
524 decomposition (i.e., heterotrophic NH_4^+ production in excess of NH_4^+ oxidation), as well as
525 NH_4^+ efflux from the sediments following organic matter remineralization (Dugdale et al.,
526 2006; Burger et al., 2020; Flynn et al., 2020). Indeed, the flow cytometry analyses indicate
527 that heterotrophic bacteria were particularly abundant throughout the water column (Fig S.2),
528 promoting NH_4^+ production.

529 While NH_4^+ should theoretically be the preferred N source to phytoplankton given its low
530 oxidation state (-3), which makes its assimilation energetically favourable (Dortch, 1990), its
531 euphotic zone concentration was too low (on average <<1 μM) to support the rates of
532 productivity observed in Elandsbaai. In contrast, high ρNO_3^- are commonly recorded for
533 phytoplankton in upwelling regions, especially when diatom- dominated (Bode et al., 1997;
534 Glover et al., 2007). In Elandsbaai, the rapid increase in ρNO_3^- within just two days of
535 upwelling, and the co-incident decline in surface NO_3^-, $Si(OH)_4$ and PO_4^{3-} concentrations, is
536 typical of the response of diatoms to a nutrient supply event (Kudela & Dugdale, 2000;
537 Fawcett & Ward, 2011). Diatoms are able to increase both their nutrient uptake and growth
538 rates very quickly, which allows them to consume a disproportionate fraction of the newly-
539 available nutrients and outpace their grazers (Fawcett & Ward, 2011; Van Oostende et al.,
540 2015; Burger et al., 2020). Diatoms can also accumulate excess NO_3^- intracellularly to use
541 when nutrients become depleted (Kudela & Dugdale, 2000). Combined, these strategies
542 allow diatoms to dominate the biomass following upwelling. Our microscopy data are
543 consistent with this idea, indicating a general dominance of diatoms throughout the
544 investigation, which strengthened post-upwelling (Fig 5).

545 Regardless of the parameters investigated (N uptake rates, NPP, chlorophyll *a*, PON,
546 POC), most of the production in the system was associated with the middle plankton size
547 class – the nanoplankton. Nanoplankton dominance has previously been observed for this
548 system, and in other upwelling regions with similar features to the SBUS (Probyn, 1992;

549 Bode et al., 1997; Burger et al., 2020). It has been suggested that this group can thrive in such
550 systems because of their intermediate size, being large enough to avoid predation but small
551 enough to remain in the euphotic zone during periods of relaxation (Burger et al., 2020),
552 which exposes them to high nutrient- and light availability. Smaller cells are also less
553 susceptible to light limitation (Finkel, 2001) and have a high affinity for nutrients, resulting
554 in a rapid growth rate (Litchman, 2007).

555 The dominance of the nanoplankton size class was at least partially reflected in the flow
556 cytometry data, which show that cryptophyte-like cells (<30 µm) followed by FC-
557 nanoplankton contributed most to biovolume. In contrast, the microscopy data indicated a
558 general higher predominance of large diatoms (>50 µm) throughout the investigation (except
559 on day 1), particularly the chain-forming *Chaetoceros* spp., with concentrations progressively
560 increasing post- upwelling. The two techniques record different phytoplankton size ranges,
561 with microscopy conducted on samples collected in a 50 µm-mesh net, while the maximum
562 cell-size that the flow cytometers could analyse was 30 µm. Nonetheless, the results of both
563 techniques support the idea of a dominant role for nanoplankton. *Chaetoceros* spp. can exist
564 as single cells (typically of ~10 µm) or as chains, and thus could have been present in both
565 the flow cytometry and microscopy samples. *Chaetoceros* spp. has been shown to dominate
566 the biomass and productivity of Elandbaai during mid-summer upwelling, which appears to
567 be due to the ability of their group to leverage the advantages of being both relatively small
568 (nanoplankton-sized single cells) and large (once aggregated as chains) (Burger et al. 2020).
569 It is likely that similar dynamics were ongoing during our late-summer investigation.

570 The $\delta^{15}N_{NO3}$ and $\delta^{18}O_{NO3}$ were high at 0m and 5m pre- and post- upwelling and
571 consistently lower (>5‰ difference) at depth and throughout the water column during
572 upwelling. The deep $\delta^{15}N_{NO3}$ of 7.3 ± 0.9‰ is slightly higher than the $\delta^{15}N_{NO3}$ of SAMW, the
573 ultimate source water to the SBUS ($\delta^{15}N_{NO3}$ = 6.6 ± 0.2‰), and similar to that of South
574 Atlantic Subtropical Mode Water (SASTMW; $\delta^{15}N_{NO3}$ = 7.2 ± 0.3‰), which derives from
575 SAMW and can also upwell in the SBUS (Flynn et al., 2020). The high $\delta^{15}N_{NO3}$ in surface

waters (11.9 ± 2.6‰) is indicative of photosynthetic NO_3^- assimilation as phytoplankton preferentially consume ^{14}N-bearing NO_3^-, leaving the residual NO_3^- pool enriched in ^{15}N (Mariotti et al., 1981; Sigman et al., 1999). The coincident rise in $\delta^{18}O_{NO3}$ in shallow waters (Fig S.3) is consistent with this interpretation as NO_3^- assimilation causes $\delta^{15}N_{NO3}$ and $\delta^{18}O_{NO3}$ to increase in unison (Granger et al., 2010). In contrast, the decline in $\delta^{18}O_{NO3}$ at depth that coincides with almost no change in $\delta^{15}N_{NO3}$ (Fig S.3) is characteristic of nitrification (i.e., NO_3^- regeneration; Flynn et al., 2020). During nitrification, the $\delta^{15}N_{NO3}$ of the produced NO_3^- is set by the $\delta^{15}N_{NO3}$ of the organic matter being remineralized (itself set by the N sources consumed by phytoplankton), while its $\delta^{18}O_{NO3}$ is set by that of water ($\delta^{18}O_{NO3}$ of ~0‰) plus an isotopic offset of ~1‰ (Sigman et al., 2009; Buchwald et al., 2012; Boshers et al., 2019). The $\delta^{15}N_{NO3}$ and $\delta^{18}O_{NO3}$ observed at depth and during upwelling could also have been influenced by coupled nitrification-denitrification at the sediment-water interface (i.e., benthic-pelagic coupling). This pathway drives a loss of low-$\delta^{15}N$-N (as N_2 gas), which raises the $\delta^{15}N$ of the remaining NO_3^- pool while coincidentally decreasing its $\delta^{18}O_{NO3}$ (Granger et al., 2011; Flynn et al., 2020). It is difficult to characterize the extent to which coupled nitrification-denitrification may have been ongoing in Elandsbaai at the time of our sampling given that the $\delta^{15}N_{NO3}$ of the bottom samples (25 m and 30 m) was ~6.6-6.9‰, which is very similar to the $\delta^{15}N_{NO3}$ of SAMW (Flynn et al., 2020). Regardless, the NO_3^- isotope data point to rapid nutrient recycling at depth, which generates high concentrations of recycled nutrients that, once supplied to the surface during mixing, can augment the offshelf (i.e., SAMW) nutrient supply, enhancing SBUS productivity (Bailey, 1991; Tyrrell & Lucas, 2002). One consequence of these dynamics, however, is a decline in bottom-water oxygen concentrations, often to hypoxic levels (Pitcher & Calder, 2000; Monteiro et al., 2011; Flynn et al., 2020).

The preferential consumption by phytoplankton of NO_3^- (over NH_4^+) was not only evident in the ρNO_3^-, but also in the $\delta^{15}N_{PON}$ of nanoplankton. This group had a $\delta^{15}N_{PON}$ in the surface layer that was ~5‰ lower than the measured $\delta^{15}N_{NO3}$ ($\delta^{15}N_{PON}$ of ~7‰, $\delta^{15}N_{NO3}$

603 of ~12‰; Fig 4). The $\delta^{15}N_{PON}$ is set by the $\delta^{15}N$ of the assimilated N sources and by the
604 extent of their consumption (Fawcett et al., 2011, 2014; Treibergs et al., 2014). Given an
605 isotope effect for NO_3^- assimilation of~5‰ (Wada & Hattori, 1978; Sigman & Fripiat, 2019),
606 our data suggest that the main N source used by nanoplankton was NO_3^- since its
607 consumption would yield PON with a $\delta^{15}N$ that was ~5‰ lower than the $\delta^{15}N_{NO3}$, as was
608 observed. In the surface layer of the ocean, NH_4^+ is generally low in $\delta^{15}N$ (<0‰) because of
609 isotope fractionation associated with the metabolic processes that result in its production
610 (Checkley & Miller, 1989). At the same time, the isotope effect of NH_4^+ assimilation appears
611 to be negligible when NH_4^+ concentrations are <5 μM (Pennock et al., 1996; Liu et al., 2013).
612 Thus, if phytoplankton were relying predominantly on NH_4^+ to fuel production, we should
613 have observed lower values of $\delta^{15}N_{PON,}$ which was not the case. We thus conclude that the
614 nanoplankton $\delta^{15}N_{PON}$ indicate sustained reliance by this size class on NO_3^-.
615 While we have almost no reliable microplankton $\delta^{15}N_{PON}$ data, the picoplankton $\delta^{15}N_{PON}$
616 was relatively high at the surface pre-upwelling and at depth post-upwelling, reaching 15‰
617 (Fig 4g). This high $\delta^{15}N_{PON}$ suggests the assimilation by picoplankton of a ^{15}N-enriched N
618 source. Since nanoplankton in upwelling systems can take up nutrients extremely rapidly
619 once they become available (Tilstone et al., 1999; Leblanc et al., 2018), outcompeting the
620 picoplankton, coupled with the fact that the higher surface area-to-volume ratio of
621 picoplankton endows them with a high affinity of low-concentration nutrients, the high
622 picoplankton $\delta^{15}N_{PON}$ may be the result of their reliance on more ^{15}N-enriched NO_3^- (i.e.,
623 following its near-complete consumption by nanoplankton when its $\delta^{15}N$ would have been
624 very high and its concentration very low). Alternately, and perhaps a more likely explanation
625 for the deeper picoplankton $\delta^{15}N_{PON}$, is that this group consumed NH_4^+ that was high in $\delta^{15}N$.
626 The partial nitrification of subsurface NH_4^+, which occurs with a large isotope effect (14-
627 19‰; Casciotti et al., 2003), generates residual NH_4^+ that can be very high in $\delta^{15}N$. The
628 assimilation of this NH_4^+ by picoplankton would result in their $\delta^{15}N_{PON}$ being similarly high
629 since NH_4^+ assimilation occurs without isotopic fractionation (Liu et al., 2013). We note,

however, that the picoplankton PON concentrations were generally very low, often falling below the methodological detention limit, such that their $\delta^{15}N_{PON}$ should be interpreted with caution. Regardless, our data strongly suggest very different nutrient acquisition strategies for nano- vs. picoplankton, which presumably contribute to their relative abundance and success in the SBUS.

In summary, the data presented above clearly record a pre-/ during / post- upwelling cycle, with NO_3^- supplied from depth being the main source of N to the (nano)phytoplankton community. This study also shows the remarkable speed of the phytoplankton response to upwelling-driven changes, with the community then returning to a pre-upwelling state within two to three days of the upwelling event.

4.2.Omega-3 production in the SBUS

As for most of the parameters investigated, TFA and omega-3 concentrations were higher pre- and post- upwelling at 0 m and 5 m, while their concentrations decreased to near-zero at depth and during upwelling, apart from bottom-water samples collected on days 4, 5 and 10 (see below). Omega-3 in the ocean are largely produced by phytoplankton (e.g., Dalsgaard et al., 2003) and we thus expected to find them in the euphotic zone during periods of relaxation. While we did observe higher omega-3 concentrations pre- and post- upwelling, our study also revealed two novel findings regarding omega-3: 1) extremely high concentrations of FA and omega-3 in SBUS phytoplankton, and 2) the speed with which the community changed from pre- to post- upwelling, and the (related) rapid production of FA and omega-3 post- upwelling.

The information available on omega-3 production for the BUS (North-BUS+SBUS) is limited (Puccinelli et al., 2021), with the only published data being the omega-3 content of suspended organic matter (1-5 μgL^{-1}) collected from a rocky shore environment in the SBUS (Puccinelli et al., 2016 b). Here, we report TFA concentrations of up to 215.5 and 175.3 μgL^{-1} and omega-3 of ~50 and ~30 μgL^{-1} pre- and post- upwelling, respectively (Fig 7). That is, we measured omega-3 concentrations that are ten-times higher than previously reported for

657 the SBUS. The discrepancy between the two studies may be due to the sampling location,
658 with Puccinelli et al. (2016b) focused on a rocky shore environment, in contrast to the open
659 water site investigated here. In Elandsbaai, elevated mixing during upwelling that supplied
660 nutrients to the surface layer favoured high omega-3 production by phytoplankton
661 immediately following upwelling, an effect that is likely limited in nearshore/rocky shore
662 regions. The magnitude of the discrepancy between the two studies is nonetheless very large.
663 The concentrations of TFA and omega-3 measured in this study are higher than those
664 observed in other EBUS, with TFA of 50-70 and 2-70 μgL^{-1} and omega-3 of 8-11 and 1-18
665 μgL^{-1} reported for the California and Humboldt upwelling systems, respectively (Gutiérrez et
666 al., 2012; Fischer et al., 2014), while no information is available for the Canary system
667 (Puccinelli et al., 2021). Among the studies investigating omega-3 production by
668 phytoplankton in EBUS, ours is the first to account for temporal variability and/or to
669 investigate the effect(s) of the upwelling cycle. Snapshot experiments will record omega-3
670 production under specific conditions only (i.e., partway through the upwelling or relaxation
671 phase). For instance, if sampling were conducted on a day of active upwelling, we would
672 have recorded omega-3 concentrations close to 0 μgL^{-1}. This value is orders of magnitude
673 lower than the concentrations we measured during the relaxation periods, such that if it were
674 taken as broadly representative of our system, it would have led us to strongly underestimate
675 omega-3 production. We thus suggest that omega-3 production in the SBUS, and in
676 upwelling systems more broadly, has previously been considerably underestimated, likely
677 due to sampling limitations.

678 The second novel finding of this work is how rapidly the phytoplankton community
679 composition changed over the upwelling cycle, and how the TFA and omega-3
680 concentrations returned to pre-upwelling levels within just two days of the upwelling event.
681 All FA analyses indicate a clear separation among samples from pre-, during and post-
682 upwelling. The pre- upwelling community was mostly characterized by non-diatom TM,
683 including haptophyte and dinoflagellate TM (together >50 % of TFA), while the post-

684 upwelling assemblage was dominated by diatom TM (>60 % of TFA; Fig 7). During
685 upwelling, no clear TM was identified. It is well known that phytoplankton community
686 composition is the main factor driving variability in FA profiles (Galloway & Winder, 2015).
687 Diatoms are usually the first phytoplankton group to proliferate post- upwelling as they are
688 NO_3^- specialists that respond rapidly to a pulse of new nutrients (Kudela & Dugdale, 2000;
689 Fawcett & Ward, 2011; Van Oostende et al., 2015) and are able to cope under variable light
690 conditions (Guerrero et al., 1981; Syrett, 1981). The diatom bloom is generally succeeded by
691 dinoflagellates, typically once the micro- and macro- nutrients essential for diatom
692 production are depleted (Martin-Jézéquel et al., 2000; Tilstone et al., 2000). Additionally
693 some dinoflagellates in the SBUS are mixotrophs, such that they can proliferate under the
694 reduced nutrient conditions typical of a post- upwelling bloom (e.g., Pitcher, 2008; van der
695 Lingen et al., 2016). Diatom TM were also present pre- upwelling, albeit at lower
696 concentrations than the non-diatom TM (20 % vs. 50 % of TFA), even though the
697 microscopy data suggest that large diatoms (>50 µm) were not abundant pre- upwelling. The
698 diatom *Chaetoceros* spp. was the main type of phytoplankton identified by microscopy and
699 was present in extremely high numbers post- upwelling (Fig 5). Since this species can occur
700 in chains and as single cells (Stoermer & Julius, 2003), it could also have been present in
701 relatively high abundances pre-upwelling but not represented in the microscopy samples.
702 While the succession of diatoms by dinoflagellates is frequently observed in upwelling
703 systems (Pitcher et al., 1991; Hansen et al., 2014; Puccinelli, et al., 2016a), the speed with
704 which the FA content of the community changed (i.e., from TFA of 131.4 μgL^{-1} on day 4, to
705 ~0 on day 6 and to 109.8 μgL^{-1} on day 8) is nonetheless remarkable. Our data suggest that
706 both diatoms and non-diatoms produce large amounts of omega-3 in Elandsbaai. The EPA
707 produced by diatoms and the DHA produced by haptophytes and dinoflagellates (Dalsgaard
708 et al., 2003; Remize et al., 2020) are the two most important omega-3 in the ocean, essential
709 for higher trophic levels including humans (Hicks et al., 2019; Tocher et al., 2019). Our study
710 shows that the dominant phytoplankton groups that proliferate immediately post- upwelling

711 and thereafter are important for omega-3 production, and additionally highlights the pivotal
712 role of upwelling in omega-3 production in the SBUS.

713 The NQI, which aims to quantify the nutritional value of a phytoplankton community
714 based on FA (Cañavate, 2019), was in the range of 216.5 ± 15.3 pre- and post- upwelling, but
715 decreased strongly at depth and during upwelling to 89.7 ± 13.5. The highest NQI values
716 derived here are similar to those reported in studies conducted in the open waters of the
717 Subtropical and Subantarctic Zones of the Southern Ocean and Antarctic coastal waters
718 (Nichols et al., 1991; Mayzaud et al., 2007; Wilson et al., 2010; Cañavate, 2019) but lower
719 than in a study conducted on the Kerguelen Plateau (Remize et al., 2022). The high
720 phytoplankton NQIs computed for Elandsbaai can be ascribed to the phytoplankton groups
721 that dominated pre- and post- upwelling (haptophytes/dinoflagellates and diatoms,
722 respectively), which are the main producers of the nutritious DHA and EPA (Dalsgaard et al.,
723 2003; Galloway & Winder, 2015; Cañavate, 2019). Our results indicate that the production of
724 both types of omega-3 was responsible for the high NQI, indicating that the phytoplankton
725 community of the SBUS constitutes a highly nutritious food source for higher trophic levels.
726 In contrast, the omega-3 concentrations recorded at depth (>10 m) and during upwelling were
727 low, generally <10 μgL^{-1} (with the exception of days 4, 5 and 10). These values can be
728 explained by the low abundance of phytoplankton, which reduced the NQI. Additionally,
729 omega-3 can easily degrade with depth or be consumed (Conte et al., 1995; Budge et al.,
730 2006), with these effects reducing the nutritional value of omega-3 available during the
731 upwelling period.

732 The high TFA and omega-3 concentrations, and NQI, observed at depth on days 4, 5 and
733 10 (Fig 7) could be linked to phytoplankton sinking and the formation of phytoplankton
734 resting spores at the sediment-water interface (Pitcher, 1986; Pitcher et al., 1991). This
735 benthic-pelagic coupling may represent an important process that supplies FA to the benthos
736 in Elandsbaai, including to the commercially relevant rock lobster, which is one of the most
737 important fisheries on South Africa's west coast (Bailey & Chapman, 1991). While this study

738 did not focus on the benthos, our results suggest that the effects of upwelling on FA
739 production may extend to benthic communities, with further studies needed to clarify the
740 connections and implications.

741 **Implications for omega-3 availability to higher trophic levels**

742 This work highlights the key role that upwelling plays in promoting a phytoplankton
743 community in the SBUS that produces high concentrations of high-quality omega-3. Indeed,
744 the measured concentrations of omega-3 were considerably higher than the current estimates
745 available for any of the EBUS. The SBUS phytoplankton community largely relied on NO_3^-
746 supplied to the surface by upwelling, indicating the presence of a tight link between new
747 NO_3^- and omega-3 production in this system. Phytoplankton form the base of the food chain
748 and are the main producers of omega-3 in the ocean, as such, investigating the relationship of
749 omega-3 concentrations to phytoplankton production with depth and over time is a suitable
750 way to evaluate the amount of omega-3 available in the system at present and in the future.

751 Current omega-3 production estimates, based mainly on meta analyses and
752 laboratory/mesocosm experiments, indicate that the global omega-3 supply may soon become
753 insufficient for a growing human population (Hixson & Arts, 2016; Colombo et al., 2020;
754 Hamilton et al., 2020), which is predicted to reach 11 billion by 2100 (Roser, 2013). The
755 results of our study indicate that this may not be the case, as we measured omega-3
756 concentrations that were 10-times higher than previous estimates from the SBUS. The
757 general lack of information available on omega-3 production in upwelling systems, combined
758 with our new concentrations for the SBUS, suggest that global omega-3 production may be
759 significantly underestimated. Similar studies focussing on the productive EBUS regions are
760 needed to better quantify the stock of omega-3 available for higher trophic levels across the
761 global ocean.

762

763 **ACKNOWLEDGEMENT**

764 This work was supported by the ISblue project, Interdisciplinary graduate school for the blue
765 planet (ANR-17-EURE-0015), co-funded by the French government under the program
766 "Investissements d'Avenir" and SAD programme fellowship to EP. Additional funding was
767 provided by the South African National Research Foundation (115335, 116142, 129320), the
768 University of Cape Town (UCT) Research Committee, and a Royal Society/African
769 Academy of Sciences Future Leaders Africa Independent *Researcher* (*FLAIR*) fellowship to
770 SF. We acknowledge the LIPIDOCEAN and the Plateforme Isotope Stable du Pôle
771 Spectrométrie Océan (PSO) at the Institut Universitaire Européen de la Mer (Plouzané,
772 France), the Marine Biogeochemistry Lab and the Stable Light Isotope Laboratory at UCT,
773 the UC Davis Stable Isotope Facility, the South African Weather Service (SAWS), and the
774 South African Department of Science and Innovation's Biogeochemistry Research
775 Infrastructure Platform (BIOGRIP). We are grateful to Pieter Truter and the Research Dive
776 Unit at UCT for their assistance at sea and members of the Fawcett research group for their
777 help with sample collection.
778

779 **CONFLICTS OF INTEREST**

780 The authors declare that they have no known competing financial interests or personal
781 relationships that could have appeared to influence the work reported in this paper.
782

783 **AUTHOR CONTRIBUTIONS**

784 EP, SF, PS conceived the ideas and designed the methodology. EP, RF, JB, HL, SW
785 collected the data. EP, RF, GD, ND, HL, CL, PS analysed the data. EP, SF, PS provided the
786 funding and resources to support the work. LP and FS contributed with critical input to the
787 interpretation of the results. EP led the writing of the manuscript. All authors contributed
788 critically to the drafts and gave final approval for publication.
789

DATA AVAILABILITY STATEMENT

The authors declare that all data relative to this work are included in the manuscript in the form of table or supplementary material. These data will also made available in a public repository with a relative DOI as part of the Data Archive System (DAS) of NIOZ once the manuscript is accepted for publication.

REFERENCES

Anderson, M. J. (2001). A new method for non-parametric multivariate analysis of variance. *Austral Ecology*, *26*(1), 32–46. https://doi.org/10.1111/j.1442-9993.2001.01070.pp.x

Aristizábal, M. F., Fewings, M. R., & Washburn, L. (2017). Effects of the Relaxation of Upwelling-Favorable Winds on the Diurnal and Semidiurnal Water Temperature Fluctuations in the Santa Barbara Channel, California. *Journal of Geophysical Research: Oceans*, *122*(10), 7958–7977. https://doi.org/10.1002/2017JC013199

Arts, M. T., Ackman, R. G., & Holub, B. J. (2001). "Essential fatty acids" in aquatic ecosystems: a crucial link between diet and human health and evolution. *Canadian Journal of Fisheries and Aquatic Sciences*, *58*(1), 122–137. https://doi.org/10.1139/f00-224

Bailey, G. W., & Chapman, P. (1991). Short-term variability during an anchor station study in the southern Benguela upwelling system: Chemical and physical oceanography. *Progress in Oceanography*, *28*(1), 9–37. https://doi.org/10.1016/0079-6611(91)90019-I

Bailey, Geoffrey W. (1991). Organic carbon flux and development of oxygen deficiency on the modern Benguela continential shelf south of 22°S: spatial and temporal variability. *Geological Society, London, Special Publications*, *58*(1), 171–183. https://doi.org/10.1144/GSL.SP.1991.058.01.12

Bode, A., Botas, J. A., & Fernández, E. (1997). Nitrate storage by phytoplankton in a coastal upwelling environment. *Marine Biology*, *129*(3), 399–406. https://doi.org/10.1007/s002270050180

Böhlke, J. K., Mroczkowski, S. J., & Coplen, T. B. (2003). Oxygen isotopes in nitrate: new reference materials for 18O:17O:16O measurements and observations on nitrate-water equilibration. *Rapid Communications in Mass Spectrometry*, *17*(16), 1835–1846. https://doi.org/10.1002/rcm.1123

Boshers, D. S., Granger, J., Tobias, C. R., Böhlke, J. K., & Smith, R. L. (2019). Constraining the Oxygen Isotopic Composition of Nitrate Produced by Nitrification. *Environmental Science & Technology*, *53*(3), 1206–1216. https://doi.org/10.1021/acs.est.8b03386

Bouvier, T., Troussellier, M., Anzil, A., Courties, C., & Servais, P. (2001). Using light scatter signal to estimate bacterial biovolume by flow cytometry. *Cytometry*, *44*(3), 188–194. https://doi.org/10.1002/1097-0320(20010701)44:3<188::AID-CYTO1111>3.0.CO;2-C

de Boyer Montégut, C., Madec, G., Fischer, A. S., Lazar, A., & Iudicone, D. (2004). Mixed layer depth over the global ocean: An examination of profile data and a profile-based climatology. *Journal of Geophysical Research: Oceans*, *109*(C12). https://doi.org/10.1029/2004JC002378

Buchwald, C., Santoro, A. E., McIlvin, M. R., & Casciotti, K. L. (2012). Oxygen isotopic composition of nitrate and nitrite produced by nitrifying cocultures and natural marine assemblages. *Limnology and Oceanography*, *57*(5), 1361–1375. https://doi.org/10.4319/lo.2012.57.5.1361

Budge, S. M., Iverson, S. J., & Koopman, H. N. (2006). Studying Trophic Ecology in Marine Ecosystems Using Fatty Acids: A Primer on Analysis and Interpretation. *Marine Mammal Science*, *22*(4), 759–801. https://doi.org/10.1111/j.1748-7692.2006.00079.x

Burger, J. M., Moloney, C. L., Walker, D. R., Parrott, R. G., & Fawcett, S. E. (2020). Drivers of short-term variability in phytoplankton production in an embayment of the southern Benguela upwelling system. *Journal of Marine Systems*, *208*, 103341. https://doi.org/10.1016/j.jmarsys.2020.103341

Cañavate, J. P. (2019). Advancing assessment of marine phytoplankton community structure and nutritional value from fatty acid profiles of cultured microalgae. *Reviews in Aquaculture*, *11*(3), 527–549. https://doi.org/10.1111/raq.12244

Carpenter, J. H. (1965). The Accuracy of the Winkler Method for Dissolved Oxygen Analysis1. *Limnology and Oceanography*, *10*(1), 135–140. https://doi.org/10.4319/lo.1965.10.1.0135

Casciotti, K. L., Sigman, D. M., Hastings, M. G., Böhlke, J. K., & Hilkert, A. (2002). Measurement of the oxygen isotopic composition of nitrate in seawater and freshwater using the denitrifier method. *Analytical Chemistry*, *74*(19), 4905–4912.

Casciotti, Karen L., Sigman, D. M., & Ward, B. B. (2003). Linking Diversity and Stable Isotope Fractionation in Ammonia-Oxidizing Bacteria. *Geomicrobiology Journal*, *20*(4), 335–353. https://doi.org/10.1080/01490450303895

Checkley, D. M., & Miller, C. A. (1989). Nitrogen isotope fractionation by oceanic zooplankton. *Deep Sea Research Part A. Oceanographic Research Papers*, *36*(10), 1449–1456. https://doi.org/10.1016/0198-0149(89)90050-2

Colombo, S. M., Rodgers, T. F. M., Diamond, M. L., Bazinet, R. P., & Arts, M. T. (2020). Projected declines in global DHA availability for human consumption as a result of global warming. *Ambio*, *49*(4), 865–880. https://doi.org/10.1007/s13280-019-01234-6

Conte, M. H., Eglinton, G., Madreira, L. A. S., Rabouille, C., Labeyrie, L., Mudge, S., et al. (1995). Origin and fate of organic biomarker compounds in the water column and sediments of the eastern North Atlantic. *Philosophical Transactions of the Royal Society of London. Series B: Biological Sciences*, *348*(1324), 169–178. https://doi.org/10.1098/rstb.1995.0059

Cury, P., & Roy, C. (1989). Optimal environmental window and pelagic fish recruitment success in upwelling areas. *Canadian Journal of Fisheries and Aquatic Sciences*, *46*(4), 670–680. https://doi.org/10.1139/f89-086

Dalsgaard, J., St. John, M., Kattner, G., Müller-Navarra, D., & Hagen, W. (2003). Fatty acid trophic markers in the pelagic marine environment. In *Advances in Marine Biology* (Vol. Volume 46, pp. 225–340). Academic Press. Retrieved from http://www.sciencedirect.com/science/article/pii/S0065288103460057

Diamond, D. (1994). QuikChem Method 10-114-21-1-B: Silicate byflow injection analysis. *Lachat Instruments*.

Dortch, Q. (1990). The interaction between ammonium and nitrate uptake in phytoplankton. *Marine Ecology Progress Series.*, *61(1)*, 183-201.

Dugdale, R. C., & Goering, J. J. (1967). Uptake of new and regenerated forms of nitrogen in primary productivity. *Limnology and Oceanography*, *12*(2), 196–206. https://doi.org/10.4319/lo.1967.12.2.0196

Dugdale, R. C., & Wilkerson, F. P. (1986). The use of 15N to measure nitrogen uptake in eutrophic oceans; experimental considerations1,2. *Limnology and Oceanography*, *31*(4), 673–689. https://doi.org/10.4319/lo.1986.31.4.0673

Dugdale, R. C., Wilkerson, F. P., Hogue, V. E., & Marchi, A. (2006). Nutrient controls on new production in the Bodega Bay, California, coastal upwelling plume. *Deep Sea Research Part II: Topical Studies in Oceanography*, *53*(25), 3049–3062. https://doi.org/10.1016/j.dsr2.2006.07.009

Fawcett, S. E., & Ward, B. B. (2011). Phytoplankton succession and nitrogen utilization during the development of an upwelling bloom. *Marine Ecology Progress Series*, *428*, 13–31. https://doi.org/10.3354/meps09070

Fawcett, Sarah E., Lomas, M. W., Casey, J. R., Ward, B. B., & Sigman, D. M. (2011). Assimilation of upwelled nitrate by small eukaryotes in the Sargasso Sea. *Nature Geoscience*, *4*(10), 717–722. https://doi.org/10.1038/ngeo1265

Fawcett, Sarah E., Lomas, M. W., Ward, B. B., & Sigman, D. M. (2014). The counterintuitive effect of summer-to-fall mixed layer deepening on eukaryotic new production in the Sargasso Sea. *Global Biogeochemical Cycles*, *28*(2), 2013GB004579. https://doi.org/10.1002/2013GB004579

Fawcett, Sarah E., Ward, B. B., Lomas, M. W., & Sigman, D. M. (2015). Vertical decoupling of nitrate assimilation and nitrification in the Sargasso Sea. *Deep Sea Research Part I: Oceanographic Research Papers*, *103*, 64–72. https://doi.org/10.1016/j.dsr.2015.05.004

Finkel, Z. V. (2001). Light absorption and size scaling of light-limited metabolism in marine diatoms. *Limnology and Oceanography*, *46*(1), 86–94. https://doi.org/10.4319/lo.2001.46.1.0086

Fischer, A. M., Ryan, J. P., Levesque, C., & Welschmeyer, N. (2014). Characterizing estuarine plume discharge into the coastal ocean using fatty acid biomarkers and pigment analysis. *Marine Environmental Research*, *99*, 106–116. https://doi.org/10.1016/j.marenvres.2014.04.006

Flynn, R. F., Granger, J., Veitch, J. A., Siedlecki, S., Burger, J. M., Pillay, K., & Fawcett, S. E. (2020). On-Shelf Nutrient Trapping Enhances the Fertility of the Southern Benguela Upwelling System. *Journal of Geophysical Research: Oceans*, *125*(6), e2019JC015948. https://doi.org/10.1029/2019JC015948

Folch, J., Lees, M., & Sloane Stanley, G. H. (1957). A simple method for the isolation and purification of total lipides from animal tissues. *The Journal of Biological Chemistry*, *226*(1), 497–509.

Galloway, A. W. E., & Winder, M. (2015). Partitioning the relative importance of phylogeny and environmental conditions on phytoplankton fatty acids. *PLOS ONE*, *10*(6), e0130053. https://doi.org/10.1371/journal.pone.0130053

Garrido, S., Rosa, R., Ben-Hamadou, R., Cunha, M. E., Chícharo, M. A., & van der Lingen, C. D. (2007). Effect of maternal fat reserves on the fatty acid composition of sardine (Sardina pilchardus) oocytes. *Comparative Biochemistry and Physiology Part B: Biochemistry and Molecular Biology*, *148*(4), 398–409. https://doi.org/10.1016/j.cbpb.2007.07.008

Glover, H. E., Garside, C., & Trees, C. C. (2007). Physiological responses of Sargasso Sea picoplankton to nanomolar nitrate perturbations. *Journal of Plankton Research*, *29*(3), 263–274. https://doi.org/10.1093/plankt/fbm013

Gonfiantini, R., Stichler, W., & Rozanski, K. (1995). Standards and intercomparison materials distributed by the International Atomic Energy Agency for stable isotope measurements. Retrieved from http://inis.iaea.org/Search/search.aspx?orig_q=RN:27021328

González-Galisteo, S., Packard, T. T., Gómez, M., Herrera, A., Dugdale, R. C., Wilkerson, F. P., et al. (2019). Calculating new production from nitrate reductase activity and light in the Peru current upwelling. *Progress in Oceanography*, *173*, 78–85. https://doi.org/10.1016/j.pocean.2019.02.009

Granger, J., Sigman, D. M., Rohde, M. M., Maldonado, M. T., & Tortell, P. D. (2010). N and O isotope effects during nitrate assimilation by unicellular prokaryotic and eukaryotic plankton cultures. *Geochimica et Cosmochimica Acta*, *74*(3), 1030–1040. https://doi.org/10.1016/j.gca.2009.10.044

Granger, J., Prokopenko, M. G., Sigman, D. M., Mordy, C. W., Morse, Z. M., Morales, L. V., et al. (2011). Coupled nitrification-denitrification in sediment of the eastern Bering Sea shelf leads to 15N enrichment of fixed N in shelf waters. *Journal of Geophysical Research: Oceans*, *116*(C11). https://doi.org/10.1029/2010JC006751

Granger, Julie, & Sigman, D. M. (2009). Removal of nitrite with sulfamic acid for nitrate N and O isotope analysis with the denitrifier method. *Rapid Communications in Mass Spectrometry*, *23*(23), 3753–3762. https://doi.org/10.1002/rcm.4307

Grasshoff, K. (1976). *Methods of Seawater Analysis*. New York: Verlag Chemie, Weinheim.

Guerrero, M. G., Vega, J. M., & Losada, M. (1981). The Assimilatory Nitrate-Reducing System and its Regulation. *Annual Review of Plant Physiology*, *32*(1), 169–204. https://doi.org/10.1146/annurev.pp.32.060181.001125

Gutiérrez, M. H., Pantoja, S., & Lange, C. B. (2012). Biogeochemical significance of fatty acid distribution in the coastal upwelling ecosystem off Concepción (36°S), Chile. *Organic Geochemistry*, *49*, 56–67. https://doi.org/10.1016/j.orggeochem.2012.05.010

Hamilton, H. A., Newton, R., Auchterlonie, N. A., & Müller, D. B. (2020). Systems approach to quantify the global omega-3 fatty acid cycle. *Nature Food*, *1*(1), 59–62. https://doi.org/10.1038/s43016-019-0006-0

Hansen, A., Ohde, T., & Wasmund, N. (2014). Succession of micro- and nanoplankton groups in ageing upwelled waters off Namibia. *Journal of Marine Systems*, *140*, 130–137. https://doi.org/10.1016/j.jmarsys.2014.05.003

Hicks, C. C., Cohen, P. J., Graham, N. A. J., Nash, K. L., Allison, E. H., D'Lima, C., et al. (2019). Harnessing global fisheries to tackle micronutrient deficiencies. *Nature*, *574*(7776), 95–98. https://doi.org/10.1038/s41586-019-1592-6

Hixson, S. M., & Arts, M. T. (2016). Climate warming is predicted to reduce omega-3, long-chain, polyunsaturated fatty acid production in phytoplankton. *Global Change Biology*, *22*(8), 2744–2755. https://doi.org/10.1111/gcb.13295

Hoch, M. P., Fogel, M. L., & Kirchman, D. L. (1992). Isotope fractionation associated with ammonium uptake by a marine bacterium. *Limnology and Oceanography*, *37*(7), 1447–1459. https://doi.org/10.4319/lo.1992.37.7.1447

Holmes, R. M., Aminot, A., Kérouel, R., Hooker, B. A., & Peterson, B. J. (1999). A simple and precise method for measuring ammonium in marine and freshwater ecosystems. *Canadian Journal of Fisheries and Aquatic Sciences*, *56*(10), 1801–1808. https://doi.org/10.1139/f99-128

Huggett, J., Verheye, H., Escribano, R., & Fairweather, T. (2009). Copepod biomass, size composition and production in the Southern Benguela: Spatio–temporal patterns of variation, and comparison with other eastern boundary upwelling systems. *Progress in Oceanography*, *83*(1), 197–207. https://doi.org/10.1016/j.pocean.2009.07.048

Hutchings, L., van der Lingen, C. D., Shannon, L. J., Crawford, R. J. M., Verheye, H. M. S., Bartholomae, C. H., et al. (2009). The Benguela Current: An ecosystem of four components. *Progress in Oceanography*, *83*(1), 15–32. https://doi.org/10.1016/j.pocean.2009.07.046

Idso, S. B., & Gilbert, R. G. (1974). On the universality of the poole and Atkins secchi disk-Light Extinction Equation. *Journal of Applied Ecology*, *11*(1), 399–401. https://doi.org/10.2307/2402029

Jónasdóttir, S. H. (2019). Fatty Acid Profiles and Production in Marine Phytoplankton. *Marine Drugs*, *17*(3). https://doi.org/10.3390/md17030151

Kirk, J. T. O. (1994). *Light and Photosynthesis in Aquatic Ecosystems* (2nd ed.). Cambridge: Cambridge University Press. https://doi.org/10.1017/CBO9780511623370

Kudela, R. M., & Dugdale, R. C. (2000). Nutrient regulation of phytoplankton productivity in Monterey Bay, California. *Deep Sea Research Part II: Topical Studies in Oceanography*, *47*(5), 1023–1053. https://doi.org/10.1016/S0967-0645(99)00135-6

Lamont, T., Hutchings, L., van den Berg, M. A., Goschen, W. S., & Barlow, R. G. (2015). Hydrographic variability in the St. Helena Bay region of the southern Benguela ecosystem. *Journal of Geophysical Research: Oceans*, *120*(4), 2920–2944. https://doi.org/10.1002/2014JC010619

Leblanc, K., Quéguiner, B., Diaz, F., Cornet, V., Michel-Rodriguez, M., Durrieu de Madron, X., et al. (2018). Nanoplanktonic diatoms are globally overlooked but play a role in spring blooms and carbon export. *Nature Communications*, *9*(1), 953. https://doi.org/10.1038/s41467-018-03376-9

van der Lingen, C. D., Hutchings, L., Lamont, T., & Pitcher, G. C. (2016). Climate change, dinoflagellate blooms and sardine in the southern Benguela Current Large Marine Ecosystem. *Environmental Development*, *17*, 230–243. https://doi.org/10.1016/j.envdev.2015.09.004

Litchman, E. (2007). CHAPTER 16 - Resource Competition and the Ecological Success of Phytoplankton. In P. G. Falkowski & A. H. Knoll (Eds.), *Evolution of Primary Producers in the Sea* (pp. 351–375). Burlington: Academic Press. https://doi.org/10.1016/B978-012370518-1/50017-5

Litzow, M. A., Bailey, K. M., Prahl, F. G., & Heintz, R. (2006). Climate regime shifts and reorganization of fish communities: the essential fatty acid limitation hypothesis. *Marine Ecology Progress Series*, *315*, 1–11. https://doi.org/10.3354/meps315001

Liu, K.-K., Kao, S.-J., Chiang, K.-P., Gong, G.-C., Chang, J., Cheng, J.-S., & Lan, C.-Y. (2013). Concentration dependent nitrogen isotope fractionation during ammonium uptake by phytoplankton under an algal bloom condition in the Danshuei estuary, northern Taiwan. *Marine Chemistry*, *157*, 242–252. https://doi.org/10.1016/j.marchem.2013.10.005

Mariotti, A., Germon, J. C., Hubert, P., Kaiser, P., Letolle, R., Tardieux, A., & Tardieux, P. (1981). Experimental determination of nitrogen kinetic isotope fractionation: Some principles; illustration for the denitrification and nitrification processes. *Plant and Soil*, *62*(3), 413–430. https://doi.org/10.1007/BF02374138

Martin-Jézéquel, V., Hildebrand, M., & Brzezinski, M. A. (2000). Silicon metabolism in diatoms: implications for growth. *Journal of Phycology*, *36*(5), 821–840. https://doi.org/10.1046/j.1529-8817.2000.00019.x

Mayzaud, P., Laureillard, J., Merien, D., Brinis, A., Godard, C., Razouls, S., & Labat, J. –P. (2007). Zooplankton nutrition, storage and fecal lipid composition in different water masses associated with the Agulhas and Subtropical Fronts. *Marine Chemistry*, *107*(2), 202–213. https://doi.org/10.1016/j.marchem.2007.07.001

Messié, M., Ledesma, J., Kolber, D. D., Michisaki, R. P., Foley, D. G., & Chavez, F. P. (2009). Potential new production estimates in four eastern boundary upwelling ecosystems. *Progress in Oceanography*, *83*(1), 151–158. https://doi.org/10.1016/j.pocean.2009.07.018

Monteiro, P. M. S., Dewitte, B., Scranton, M. I., Paulmier, A., & Plas, A. K. van der. (2011). The role of open ocean boundary forcing on seasonal to decadal-scale variability and long-term change of natural shelf hypoxia. *Environmental Research Letters*, *6*(2), 025002. https://doi.org/10.1088/1748-9326/6/2/025002

Mourente, G. (2003). *Accumulation of DHA (docosahexaenoic acid; 22:6n-3) in larval and juvenile fish brain*. Bergen (2003.

Nichols, P. D., Skerratt, J. H., Davidson, A., Burton, H., & Mcmeekin, T. A. (1991). Lipids of cultured Phaeocystis pouchetii: Signatures for food-web, biogeochemical and environmental studies in Antarctica and the Southern ocean. *Phytochemistry*, *30*(10), 3209–3214. https://doi.org/10.1016/0031-9422(91)83177-M

Parrish, C. C., Abrajano, T. A., Budge, S. M., Helleur, R. J., Hudson, E. D., Pulchan, K., & Ramos, C. (2000). Lipid and phenolic biomarkers in marine ecosystems: analysis and applications. In P. J. Wangersky (Ed.), *Marine Chemistry* (pp. 193–223). Springer Berlin Heidelberg. Retrieved from http://link.springer.com/chapter/10.1007/10683826_8

Parrish, Christopher C. (2013, April 22). Lipids in Marine Ecosystems [Review Article]. https://doi.org/10.5402/2013/604045

Parsons, T. R., Maita, Y., & Lalli, C. M. (1984). *A Manual of Chemical & Biological Methods for Seawater Analysis*. Elsevier. https://doi.org/10.1016/C2009-0-07774-5

Pauly, D., & Christensen, V. (1995). Primary production required to sustain global fisheries. *Nature*, *374*(6519), 255–257. https://doi.org/10.1038/374255a0

Pennock, J. R., Velinsky, D. J., Ludlam, J. M., Sharp, J. H., & Fogel, M. L. (1996). Isotopic fractionation of ammonium and nitrate during uptake by Skeletonema costatum: Implications for δ15N dynamics under bloom conditions. *Limnology and Oceanography*, *41*(3), 451–459. https://doi.org/10.4319/lo.1996.41.3.0451

Pitcher, G. C. (1986). Sedimentary flux and the formation of resting spores of selected Chaetoceros species at two sites in the southern Benguela System. *South African Journal of Marine Science*, *4*(1), 231–244. https://doi.org/10.2989/025776186784461657

Pitcher, G. C. (2008). Contrasting bays and red tides in the southern Benguela upwelling system. *Oceanography*, *21*(3), 82.

Pitcher, G. C., & Calder, D. (2000). Harmful algal blooms of the southern Benguela Current: a review and appraisal of monitoring from 1989 to 1997. *South African Journal of Marine Science*, *22*(1), 255–271. https://doi.org/10.2989/025776100784125681

Pitcher, G. C., Walker, D. R., Mitchell-Innes, B. A., & Moloney, C. L. (1991). Short-term variability during an anchor station study in the southern Benguela upwelling system: phytoplankton dynamics. *Progress in Oceanography*, *28*(1–2), 39–64. https://doi.org/10.1016/0079-6611(91)90020-M

Probyn, T. A. (1992). The inorganic nitrogen nutrition of phytoplankton in the southern Benguela: new production, phytoplankton size and implications for pelagic foodwebs. *South African Journal of Marine Science*, *12*(1), 411–420. https://doi.org/10.2989/02577619209504715

Probyn, T. A., & Painting, S. J. (1985). Nitrogen uptake by size-fractionated phytoplankton populations in Antarctic surface waters. *Limnology and Oceanography*, *30*(6), 1327–1332. https://doi.org/10.4319/lo.1985.30.6.1327

Puccinelli, E, Noyon, M., & McQuaid, C. (2016). Hierarchical effects of biogeography and upwelling shape the dietary signatures of benthic filter feeders. *Marine Ecology Progress Series*. https://doi.org/10.3354/meps11567

Puccinelli, E., McQuaid, C. D., & Noyon, M. (2016). Spatio-temporal variation in effects of upwelling on the fatty acid composition of benthic filter feeders in the Southern Benguela Ecosystem: not all upwelling Is equal. *PLOS ONE*, *11*(8), e0161919. https://doi.org/10.1371/journal.pone.0161919

Puccinelli, Eleonora, Sardenne, F., Pecquerie, L., Fawcett, S. E., Machu, E., & Soudant, P. (2021). Omega-3 Pathways in Upwelling Systems: The Link to Nitrogen Supply. *Frontiers in Marine Science*, *8*. https://doi.org/10.3389/fmars.2021.664601

Ravet, J. L., Brett, M. T., & Arhonditsis, G. B. (2010). The effects of seston lipids on zooplankton fatty acid composition in Lake Washington, Washington, USA. *Ecology*, *91*(1), 180–190.

Remize, M., Planchon, F., Loh, A. N., Grand, F. L., Bideau, A., Goic, N. L., et al. (2020). Study of Synthesis Pathways of the Essential Polyunsaturated Fatty Acid 20:5n-3 in the Diatom Chaetoceros Muelleri Using 13C-Isotope Labeling. *Biomolecules*, *10*(5), 797. https://doi.org/10.3390/biom10050797

Remize, M., Planchon, F., Loh, A. N., Le Grand, F., Bideau, A., Puccinelli, E., et al. (2022). Origin and fate of long-chain polyunsaturated fatty acids in the Kerguelen Islands region (Southern Ocean) in late summer. *Journal of Marine Systems*, *228*, 103693. https://doi.org/10.1016/j.jmarsys.2021.103693

Roser, M. (2013). Future Population Growth. *Our World in Data*. Retrieved from https://ourworldindata.org/future-population-growth

Saxberg, B. E., & Kowalski, B. R. (1979). Generalized standard addition method. *Analytical Chemistry*, *51*(7), 1031–1038.

Shannon, L. (1985). The Benguela ecosystem. I: Evolution of the Benguela physical features and processes. *Undefined*. Retrieved from https://www.semanticscholar.org/paper/The-Benguela-ecosystem.-I%3A-Evolution-of-the-and-Shannon/264dec3872d80bea3a33909e1e8509c9b81d6dda

Shannon, L. V., & Nelson, G. (1996). The Benguela: large scale features and processes and system variability. In *The South Atlantic* (pp. 163–210). Springer Berlin Heidelberg. Retrieved from http://link.springer.com/chapter/10.1007/978-3-642-80353-6_9

Sigman, D. M., & Fripiat, F. (2019). Nitrogen Isotopes in the Ocean. In J. K. Cochran, H. J. Bokuniewicz, & P. L. Yager (Eds.), *Encyclopedia of Ocean Sciences (Third Edition)* (pp. 263–278). Oxford: Academic Press. https://doi.org/10.1016/B978-0-12-409548-9.11605-7

Sigman, D. M., Altabet, M. A., McCorkle, D. C., Francois, R., & Fischer, G. (1999). The $\delta^{15}N$ of nitrate in the southern ocean: Consumption of nitrate in surface waters. *Global Biogeochemical Cycles*, *13*(4), 1149–1166. https://doi.org/10.1029/1999GB900038

Sigman, D. M., Casciotti, K. L., Andreani, M., Barford, C., Galanter, M., & Böhlke, J. K. (2001). A bacterial method for the nitrogen isotopic analysis of nitrate in seawater and freshwater. *Analytical Chemistry*, *73*(17), 4145–4153. https://doi.org/10.1021/ac010088e

Sigman, Daniel M., DiFiore, P. J., Hain, M. P., Deutsch, C., Wang, Y., Karl, D. M., et al. (2009). The dual isotopes of deep nitrate as a constraint on the cycle and budget of oceanic fixed nitrogen. *Deep Sea Research Part I: Oceanographic Research Papers*, *56*(9), 1419–1439. https://doi.org/10.1016/j.dsr.2009.04.007

Smayda, T. J., & Trainer, V. L. (2010). Dinoflagellate blooms in upwelling systems: Seeding, variability, and contrasts with diatom bloom behaviour. *Progress in Oceanography*, *85*(1–2), 92–107. https://doi.org/10.1016/j.pocean.2010.02.006

Stoermer, E. F., & Julius, M. L. (2003). 15 - CENTRIC DIATOMS. In J. D. Wehr & R. G. Sheath (Eds.), *Freshwater Algae of North America* (pp. 559–594). Burlington: Academic Press. https://doi.org/10.1016/B978-012741550-5/50016-7

Syrett, J. P. (1981). Nitrogen metabolism of microalgae. *Can. Bull. Fish. Aquat. Sci.*, *210*, 182–210.

Tacon, A. G. J., & Metian, M. (2009). Fishing for Feed or Fishing for Food: Increasing Global Competition for Small Pelagic Forage Fish. *Ambio*, *38*(6), 294–302. https://doi.org/10.2307/40390239

Tilstone, G., Míguez, B., Figueiras, F., & Fermín, E. (2000). Diatom dynamics in a coastal ecosystem affected by upwelling: coupling between species succession, circulation and biogeochemical processes. *Marine Ecology Progress Series*, *205*, 23–41. https://doi.org/10.3354/meps205023

Tilstone, G. H., Figueiras, F. G., Fermín, E. G., & Arbones, B. (1999). Significance of nanophytoplankton photosynthesis and primary production in a coastal upwelling system (Ría de Vigo, NW Spain). *Marine Ecology Progress Series*, *183*, 13–27. https://doi.org/10.3354/meps183013

Tocher, D. R. (2015). Omega-3 long-chain polyunsaturated fatty acids and aquaculture in perspective. *Aquaculture*, *449*, 94–107. https://doi.org/10.1016/j.aquaculture.2015.01.010

Tocher, D. R., Betancor, M. B., Sprague, M., Olsen, R. E., & Napier, J. A. (2019). Omega-3 Long-Chain Polyunsaturated Fatty Acids, EPA and DHA: Bridging the Gap between Supply and Demand. *Nutrients*, *11*(1), 89. https://doi.org/10.3390/nu11010089

Treibergs, L. A., Fawcett, S. E., Lomas, M. W., & Sigman, D. M. (2014). Nitrogen isotopic response of prokaryotic and eukaryotic phytoplankton to nitrate availability in Sargasso Sea surface waters. *Limnology and Oceanography*, *59*(3), 972–985. https://doi.org/10.4319/lo.2014.59.3.0972

Tyrrell, T., & Lucas, M. I. (2002). Geochemical evidence of denitrification in the Benguela upwelling system. *Continental Shelf Research*, *22*(17), 2497–2511. https://doi.org/10.1016/S0278-4343(02)00077-8

Van Oostende, N., Dunne, J. P., Fawcett, S. E., & Ward, B. B. (2015). Phytoplankton succession explains size-partitioning of new production following upwelling-induced blooms. *Journal of Marine Systems*, *148*, 14–25. https://doi.org/10.1016/j.jmarsys.2015.01.009

Wada, E., & Hattori, A. (1978). Nitrogen isotope effects in the assimilation of inorganic nitrogenous compounds by marine diatoms. *Geomicrobiology Journal*, *1*(1), 85–101. https://doi.org/10.1080/01490457809377725

Waldron, H. N., & Probyn, T. A. (1992). Nitrate supply and potential new production in the Benguela upwelling system. *South African Journal of Marine Science*, *12*(1), 29–39. https://doi.org/10.2989/02577619209504688

Ward, T. M., Mcleay, L. J., Dimmlich, W. F., Rogers, P. J., Mcclatchie, S., Matthews, R., et al. (2006). Pelagic ecology of a northern boundary current system: effects of upwelling on the production and distribution of sardine (*Sardinops sagax*), anchovy (*Engraulis australis*) and southern bluefin tuna (*Thunnus maccoyii*) in the Great Australian Bight. *Fisheries Oceanography*, *15*(3), 191–207. https://doi.org/10.1111/j.1365-2419.2006.00353.x

Welschmeyer, N. A. (1994). Fluorometric analysis of chlorophyll a in the presence of chlorophyll b and pheopigments. *Limnology and Oceanography*, *39*(8), 1985–1992. https://doi.org/10.4319/lo.1994.39.8.1985

Wilson, S. E., Steinberg, D. K., Chu, F.-L. E., & Bishop, J. K. B. (2010). Feeding ecology of mesopelagic zooplankton of the subtropical and subarctic North Pacific Ocean determined with fatty acid biomarkers. *Deep Sea Research Part I: Oceanographic Research Papers*, *57*(10), 1278–1294. https://doi.org/10.1016/j.dsr.2010.07.005

Zhang, Y., Bellingham, J. G., Ryan, J. P., & Godin, M. A. (2015). Evolution of a physical and biological front from upwelling to relaxation. *Continental Shelf Research*, *108*, 55–64. https://doi.org/10.1016/j.csr.2015.08.005